

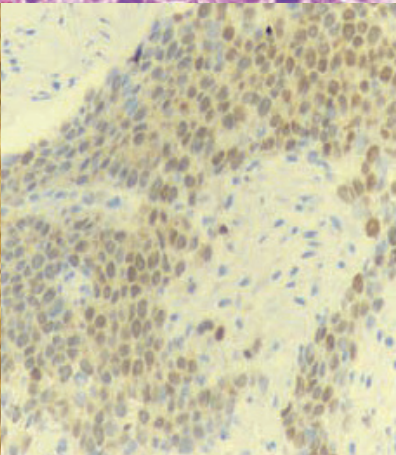
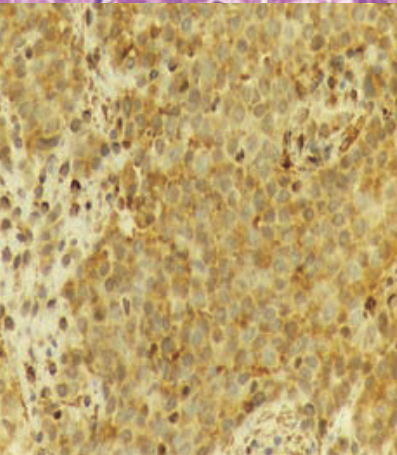
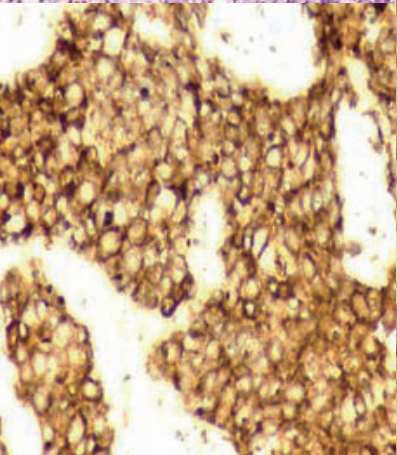
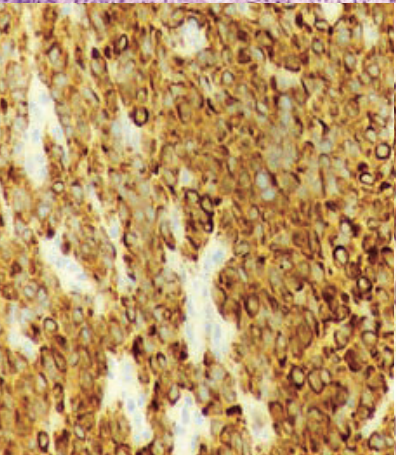
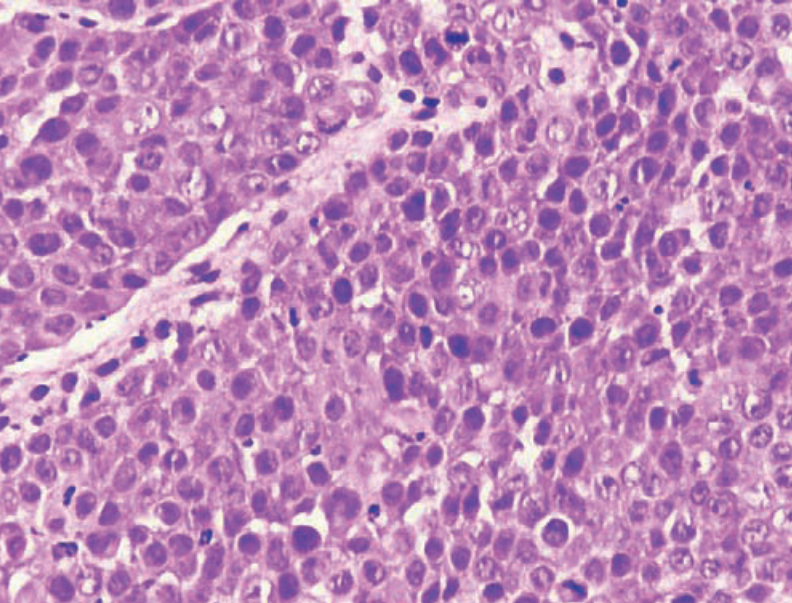
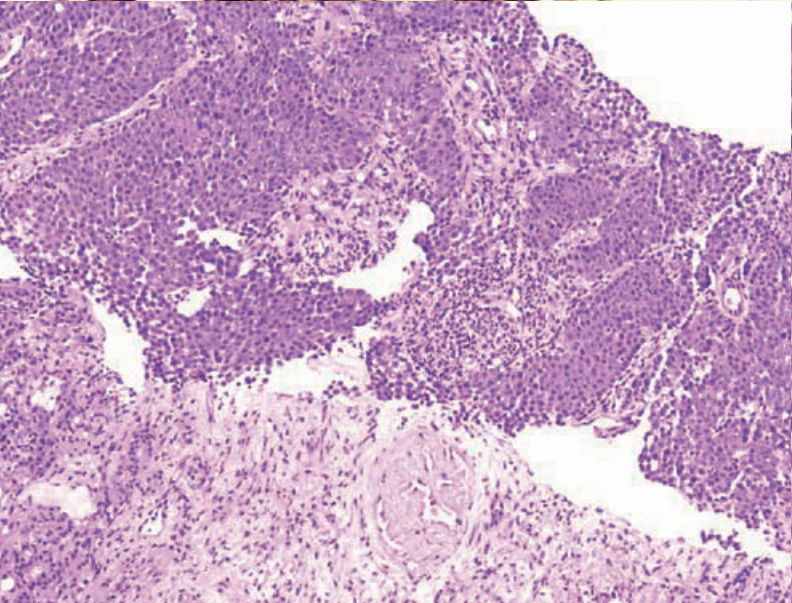
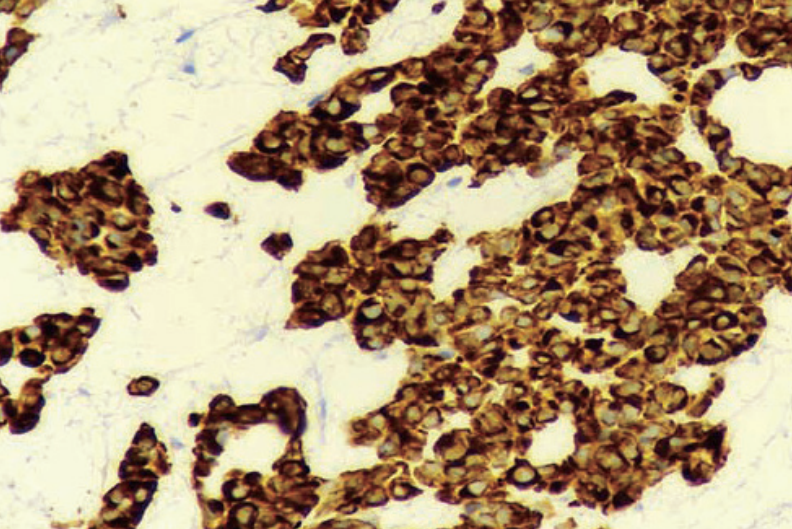
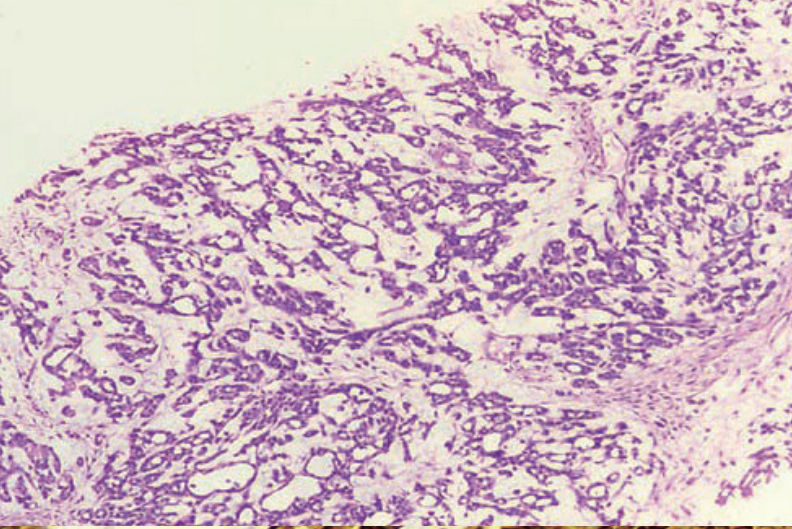
# JPTM

Journal of Pathology  
and Translational Medicine

September 2023  
Vol. 57 / No.5  
jpatholm.org  
pISSN: 2383-7837  
eISSN: 2383-7845



***EWSR1 Rearranged  
Renal Myoepithelial  
Carcinoma***



## Aims & Scope

The *Journal of Pathology and Translational Medicine* is an open venue for the rapid publication of major achievements in various fields of pathology, cytopathology, and biomedical and translational research. The Journal aims to share new insights into the molecular and cellular mechanisms of human diseases and to report major advances in both experimental and clinical medicine, with a particular emphasis on translational research. The investigations of human cells and tissues using high-dimensional biology techniques such as genomics and proteomics will be given a high priority. Articles on stem cell biology are also welcome. The categories of manuscript include original articles, review and perspective articles, case studies, brief case reports, and letters to the editor.

## Subscription Information

To subscribe to this journal, please contact the Korean Society of Pathologists/the Korean Society for Cytopathology. Full text PDF files are also available at the official website (<https://jpatholm.org>). *Journal of Pathology and Translational Medicine* is indexed by Emerging Sources Citation Index (ESCI), PubMed, PubMed Central, Scopus, KoreaMed, KoMCI, WPRIM, Directory of Open Access Journals (DOAJ), and CrossRef. Circulation number per issue is 50.

## Editors-in-Chief

Jung, Chan Kwon, MD (*The Catholic University of Korea, Korea*) <https://orcid.org/0000-0001-6843-3708>

Park, So Yeon, MD (*Seoul National University, Korea*) <https://orcid.org/0000-0002-0299-7268>

## Associate Editors

Bychkov, Andrey, MD (*Kameda Medical Center, Japan; Nagasaki University Hospital, Japan*) <https://orcid.org/0000-0002-4203-5696>

Kim, Haeryoung, MD (*Seoul National University, Korea*) <https://orcid.org/0000-0002-4205-9081>

Lee, Hee Eun, MD (*Mayo Clinic, USA*) <https://orcid.org/0000-0001-6335-7312>

Shin, Eunah, MD (*Yongin Severance Hospital, Yonsei University, Korea*) <https://orcid.org/0000-0001-5961-3563>

## Editorial Board

Avila-Casado, Maria del Carmen, MD (*University of Toronto, Toronto General Hospital UHN, Canada*)

Bae, Jeong Mo, MD (*Seoul National University, Korea*)

Bae, Young Kyung, MD (*Yeungnam University, Korea*)

Bongiovanni, Massimo, MD (*Lausanne University Hospital, Switzerland*)

Bova, G. Steven, MD (*University of Tampere, Finland*)

Choi, Joon Hyuk, MD (*Yeungnam University, Korea*)

Chong, Yo Sep, MD (*The Catholic University of Korea, Korea*)

Chung, Jin-Haeng, MD (*Seoul National University, Korea*)

Fadda, Guido, MD (*Catholic University of Rome-Foundation Agostino Gemelli University Hospital, Italy*)

Fukushima, Noriyoshi, MD (*Jichi Medical University, Japan*)

Go, Heounjeong, MD (*University of Ulsan, Korea*)

Hong, Soon Won, MD (*Yonsei University, Korea*)

Jain, Deepali, MD (*All India Institute of Medical Sciences, India*)

Kakudo, Kennichi, MD (*Izumi City General Hospital, Japan*)

Kim, Jang-Hee, MD (*Ajou University, Korea*)

Kim, Jung Ho, MD (*Seoul National University, Korea*)

Kim, Se Hoon, MD (*Yonsei University, Korea*)

Komuta, Mina, MD (*Keio University, Tokyo, Japan*)

Kwon, Ji Eun, MD (*Ajou University, Korea*)

Lai, Chiung-Ru, MD (*Taipei Veterans General Hospital, Taiwan*)

Lee, C. Soon, MD (*University of Western Sydney, Australia*)

Lee, Hwajeong, MD (*Albany Medical College, USA*)

Lee, Sung Hak, MD (*The Catholic University, Korea*)

Liu, Zhiyan, MD (*Shanghai Jiao Tong University, China*)

Lkhagvadorj, Sayamaa, MD

(*Mongolian National University of Medical Sciences, Mongolia*)

Moran, Cesar, MD (*MD Anderson Cancer Center, U.S.A.*)

Paik, Jin Ho, MD (*Seoul National University, Korea*)

Park, Jeong Hwan, MD (*Seoul National University, Korea*)

Sakhuja, Pujja, MD (*Govind Ballabh Pant Hospital, India*)

Shahid, Pervez, MD (*Aga Khan University, Pakistan*)

Song, Joon Seon, MD (*University of Ulsan, Korea*)

Tan, Puay Hoon, MD (*National University of Singapore, Singapore*)

Than, Nandor Gabor, MD (*Semmelweis University, Hungary*)

Tse, Gary M., MD (*The Chinese University of Hong Kong, Hong Kong*)

Yatabe, Yasushi, MD (*Aichi Cancer Center, Japan*)

Zhu, Yun, MD (*Jiangsu Institution of Nuclear Medicine, China*)

## Ethic Editor

Choi, In-Hong, MD (*Yonsei University, Korea*)

Huh, Sun, MD (*Hallym University, Korea*)

## Statistics Editors

Kim, Dong Wook (*National Health Insurance Service Ilsan Hospital, Korea*)

Lee, Hye Sun (*Yonsei University, Korea*)

## Manuscript Editor

Chang, Soo-Hee (*InfoLumi Co., Korea*)

## Layout Editor

Kim, Haeja (*iMiS Company Co., Ltd., Korea*)

## Website and JATS XML File Producers

Cho, Yoosang (*M2Community Co., Korea*)

Im, Jeonghee (*M2Community Co., Korea*)

## Administrative Assistants

Kim, Da Jeong (*The Korean Society of Pathologists*)

Jeon, Anmi (*The Korean Society for Cytopathology*)

## Contact the Korean Society of Pathologists/the Korean Society for Cytopathology

**Publishers:** Choe, Gheeyoung, MD, Lee, Seung-Sook, MD

**Editors-in-Chief:** Jung, Chan Kwon, MD, Park, So Yeon, MD

**Published by the Korean Society of Pathologists/the Korean Society for Cytopathology**

### Editorial Office

Room 1209 Gwanghwamun Officia, 92 Saemunan-ro, Jongno-gu, Seoul 03186, Korea

Tel: +82-2-795-3094 Fax: +82-2-790-6635 E-mail: [office@jpatholm.org](mailto:office@jpatholm.org)

#1508 Renaissancetower, 14 Mallijae-ro, Mapo-gu, Seoul 04195, Korea

Tel: +82-2-593-6943 Fax: +82-2-593-6944 E-mail: [office@jpatholm.org](mailto:office@jpatholm.org)

**Printed by** iMiS Company Co., Ltd. (JMC)

Jungang Bldg. 18-8 Wonhyo-ro 89-gil, Yongsan-gu, Seoul 04314, Korea

Tel: +82-2-717-5511 Fax: +82-2-717-5515 E-mail: [ml@smileml.com](mailto:ml@smileml.com)

**Manuscript Editing by** InfoLumi Co.

210-202, 421 Pangyo-ro, Bundang-gu, Seongnam 13522, Korea

Tel: +82-70-8839-8800 E-mail: [infolumi.chang@gmail.com](mailto:infolumi.chang@gmail.com)

Front cover image: Histologic and immunohistochemical features of EWSR1 rearranged renal myoepithelial carcinoma (p.285, 286).

© Copyright 2023 by the Korean Society of Pathologists/the Korean Society for Cytopathology

© Journal of Pathology and Translational Medicine is an Open Access journal under the terms of the Creative Commons Attribution Non-Commercial License (<https://creativecommons.org/licenses/by-nc/4.0>).

© This paper meets the requirements of KS X ISO 9706, ISO 9706-1994 and ANSI/NISO Z.39.48-1992 (Permanence of Paper).

## CONTENTS

---

### ORIGINAL ARTICLES

- 251 Diagnostic proficiency test using digital cytopathology and comparative assessment of whole slide images of cytologic samples for quality assurance program in Korea

Yosep Chong, Soon Auck Hong, Hoon Kyu Oh, Soo Jin Jung, Bo-Sung Kim, Ji Yun Jeong, Ho-Chang Lee, Gyungyub Gong, The Committee of Quality Improvement of Korean Society for Cytopathology

- 265 Establishing molecular pathology curriculum for pathology trainees and continued medical education: a collaborative work from The Molecular Pathology Study Group of the Korean Society of Pathologists

Jiwon Koh, Ha Young Park, Jeong Mo Bae, Jun Kang, Uiju Cho, Seung Eun Lee, Haeyoun Kang, Min Eui Hong, Jae Kyung Won, Youn-La Choi, Wan-Seop Kim, Ahwon Lee, The Molecular Pathology Study Group of the Korean Society of Pathologists

### CASE REPORTS

- 273 Hepatic small vessel neoplasm: not totally benign, not yet malignant

Madison Miranda, David Howell, Tony El Jabbour

- 278 Diagnostic conundrums of schwannomas: two cases highlighting morphological extremes and diagnostic challenges in biopsy specimens of soft tissue tumors

Chankyung Kim, Yang-Guk Chung, Chan Kwon Jung

- 284 *EWSR1* rearranged primary renal myoepithelial carcinoma: a diagnostic conundrum

Nilay Nishith, Zachariah Chowdhury

# Diagnostic proficiency test using digital cytopathology and comparative assessment of whole slide images of cytologic samples for quality assurance program in Korea

Yosep Chong<sup>1</sup>, Soon Auck Hong<sup>2</sup>, Hoon Kyu Oh<sup>3</sup>, Soo Jin Jung<sup>4</sup>, Bo-Sung Kim<sup>5</sup>, Ji Yun Jeong<sup>6</sup>, Ho-Chang Lee<sup>7</sup>, Gyungyub Gong<sup>8</sup>,  
 The Committee of Quality Improvement of Korean Society for Cytopathology

<sup>1</sup>Department of Hospital Pathology, College of Medicine, The Catholic University of Korea, Seoul;

<sup>2</sup>Department of Pathology, Chung-Ang University College of Medicine, Seoul;

<sup>3</sup>Department of Pathology, Daegu Catholic University School of Medicine, Daegu;

<sup>4</sup>Department of Pathology, Inje University Busan Paik Hospital, Busan;

<sup>5</sup>Department of Pathology, Green Cross Laboratories, Yongin;

<sup>6</sup>Department of Pathology, Kyungpook National University Chilgok Hospital, School of Medicine, Kyungpook National University, Daegu;

<sup>7</sup>Department of Pathology, Chungbuk National University College of Medicine, Cheongju;

<sup>8</sup>Department of Pathology, Asan Medical Center, University of Ulsan College of Medicine, Seoul, Korea

**Background:** The Korean Society for Cytopathology introduced a digital proficiency test (PT) in 2021. However, many doubtful opinions remain on whether digitally scanned images can satisfactorily present subtle differences in the nuclear features and chromatin patterns of cytological samples. **Methods:** We prepared 30 whole-slide images (WSIs) from the conventional PT archive by a selection process for digital PT. Digital and conventional PT were performed in parallel for volunteer institutes, and the results were compared using feedback. To assess the quality of cytological assessment WSIs, 12 slides were collected and scanned using five different scanners, with four cytopathologists evaluating image quality through a questionnaire. **Results:** Among the 215 institutes, 108 and 107 participated in glass and digital PT, respectively. No significant difference was noted in category C (major discordance), although the number of discordant cases was slightly higher in the digital PT group. Leica, 3DHitech Panoramic 250 Flash, and Hamamatsu NanoZoomer 360 systems showed comparable results in terms of image quality, feature presentation, and error rates for most cytological samples. Overall satisfaction was observed with the general convenience and image quality of digital PT. **Conclusions:** As three-dimensional clusters are common and nuclear/chromatin features are critical for cytological interpretation, careful selection of scanners and optimal conditions are mandatory for the successful establishment of digital quality assurance programs in cytology.

**Key Words:** Cytology; Quality assurance; Digital pathology; Whole-slide image; Whole-slide scanner

**Received:** May 24, 2023 **Revised:** July 11, 2023 **Accepted:** July 17, 2023

**Corresponding Author:** Yosep Chong, MD, PhD, Department of Hospital Pathology, Uijeongbu St. Mary's Hospital, College of Medicine, The Catholic University of Korea, 271 Cheonbo-ro, Uijeongbu 11765, Korea

Tel: +82-31-820-3160, Fax: +82-31-820-3877, E-mail: ychong@catholic.ac.kr

Continuous Quality Improvement (CQI) program of the Korean Society for Cytopathology (KSC) program began in 1995 and consists of four rounds of annual external quality assurance programs (QAP): 1, an annual survey of the statistics of cytopathological examinations; 2, sample adequacy evaluation test; 3, submission of candidate slides for diagnostic proficiency test (PT); and 4, diagnostic PT performed using five glass slides from each laboratory (two gynecologic samples [GYN], two body fluids [BF], and one fine-needle aspiration cytology [FNAC] sample)

[1-4]. In 2020, the KSC CQI program started introducing a digital proficiency test (DPT) owing to various problems with conventional diagnostic PT using glass slides [2,3].

As of 2019, 208 cytopathology laboratories in Korea have participated in this QAP, reporting over 10 million cytopathological examinations nationwide, and diagnostic PT has been performed using 1,081 glass slides [5,6]. In 2018, the Committee of CQI of the KSC introduced an online management system to collect statistics and PT results to handle the general QAP

(Supplementary Fig. S1) [6,7]. The CQI KSC has successfully increased the sample adequacy, reduced the number of major discordant cases among cytology–histology correlation reviews (CHCR) of internal QAP (from 1.6% to 0.5%), and increased the concordance rate in diagnostic PT during the last two decades with all these efforts in conjunction with the National Cancer Screening Program [2,6].

However, the current PT using glass slides is accompanied with an insufficient supply of test slides from the participating laboratories, time- and labor-intensive work of eligibility assessment, risk of damage or loss of glass slides during transportation, risk of patient personal information leakage, impaired credibility of a few cases, unequal distribution of QAP cases, and storage-associated problems such as discoloration and contamination. Thereafter, the KSC decided to adopt a digital pathology technology for PT in 2021 [2,8]. Because many doubtful opinions remain on whether digitally scanned images can deliver subtle differences in nuclear features and chromatin patterns of cytologic samples satisfactorily, ensuring the quality of test slides for diagnostic PT is important. However, the international QAPs that started digital diagnostic PT, such as the UK National External Quality Assessment Service (NEQAS) and Royal College of Pathologists of Australia QAP (RCPAQAP), are still in their elementary stage, and a comparative analysis of the image quality of the cytologic slides according to the scanners and optimized scanning conditions has not been fully explored [9,10].

Here, we present the results and feedback of diagnostic DPT during 2021 and 2022 and a comparative assessment of the whole-slide images of cytologic samples for QAP according to the major vendors of whole-slide scanners. We performed a comprehensive comparative assessment of whole-slide images of various cytologic samples using different scanners under various scanning conditions to find an optimal image quality of cytologic slides for digital QAP and provide background information on the choice of digital pathology systems appropriate for cytopathologic practice.

## MATERIALS AND METHODS

### Parallel digital pathology and glass PTs and post-test feedback survey

Annually, more than 1,000 glass slides were collected by the KSC from the donation of participating institutes/hospital in South Korea. Out of 7,000 slides of the PT archive, we initially selected 258 slides and 85 slides were chosen and scanned after the first round of review by the KSC CQI members. The 85 scanned

images were carefully reviewed by five KSC board members and only 30 WSIs were finally selected for the digital PT. Digital and conventional PT were performed in parallel for volunteer institutes among the 215 registered cytopathology laboratories in South Korea, and the results were compared with feedback. Conventional PT was performed using five glass slides, including two gynecology (Pap smear), one body fluid, one urine, and one FNAC sample. Digital PT was performed using six whole slide cytologic images, including two gynecology, two body fluids, one urine, and one FNAC sample. The diagnostic concordance between the cytological diagnosis submitted by the institutes and the original diagnosis of the histologically confirmed case was categorized as either concordant (category O) or one of the three discordant categories: category A (minimal clinical impact), category B (minor clinical impact), or category C (major clinical impact). The criteria for discordance assessment according to sample type were developed by the CQI KSC and provided to each institute (Supplementary Table S1–S3).

### Comparative assessment of whole-slide images of cytologic samples based on scanners

For the comparative assessment of cytological assessment WSIs, 12 cytopathology slides were selected after careful review out of the PT archive independently to the PT. The scanning of these 12 cytological slide was performed using five different scanners from major scanner vendors. Each system utilizes its own specific image viewer software, it applies to the scanning of glass slides and the accompanying image viewer software provided by each scanner used under various scanning conditions (Table 1, Supplementary Fig. S1). For instance, AT2 (Leica Biosystems, Nussloch, Germany) utilizes ImageScope, Flash 250 III (3DHitech, Budapest, Hungary) employs SlideViewer, NanoZoomer S360 (Hamamatsu, Japan) utilizes NDP.view2, and Ventana DP200 (Roche, Basel, Switzerland) operates with uPath software. Since the IMS viewer of the Ultra-Fast Scanner (Philips, Amsterdam, Netherlands) was unavailable, we utilized the Pathomation image viewer instead. Scanner specifications, such as capacity, z-stacking, file format, size, scan time, and error rate, were assessed. Four cytopathologists assessed image quality using a questionnaire on focus, color balance, nuclear/cytoplasmic/chromatin features, etc., using different monitors and workstations of their own (Table 2). The questionnaire consisted of 17 questions that evaluated the quality of the scanned image of a tissue sample. The questions assessed the evenness of the magnification, white balance, and color of the image, as well as the clarity of the focus and ability to differentiate cells and artifacts. Additionally, questions focused on the

**Table 1.** Selected slides for image quality comparison

Label	Specimen type	Diagnosis	Z-stacking	Layers
C16-092	Pap smear (conventional)	Squamous cell carcinoma	Yes	5
C16-223	Pap smear (conventional)	High grade squamous intraepithelial lesion	Yes	5
C-16-141	Pap smear (LBP)	Low grade squamous intraepithelial lesion	No	1
C-16-005	Pap smear (LBP)	Adenocarcinoma	No	1
R-17-009	Bronchial washing	Squamous cell carcinoma	Yes	3
R-18-037	Sputum	Squamous cell carcinoma	Yes	3
BF-17-016	Pleural fluid	Adenocarcinoma	Yes	3
BF-17-004	Ascitic fluid	Serous carcinoma, metastatic	No	1
U-17-030	Urine cytology	Papillary urothelial carcinoma, non-invasive, high grade	Yes	3
ABC-18-006	Thyroid FNA	Papillary carcinoma	Yes	3
ABC-17-182	Salivary FNA	Pleomorphic adenoma	Yes	3
ABC-17-197	Lymph node FNA	Metastatic carcinoma (breast)	Yes	3

LBP, liquid-based preparation; FNA, fine-needle aspiration.

**Table 2.** Questionnaire for image quality assessment

No.	Questions	1	2	3
1	All the area of the slide were scanned properly?	All	Partly no (<10%)	No (>10%)
2	The scanned image show even magnification in all the area?	Yes	Partly no	No
3	The white balance of the background image is appropriate?	Yes	Partly no	No
4	Is the focus of the image even enough throughout the image?	Yes	Partly no	No
5	Is it easy to differentiate cells and background artifacts such as inflammatory cells and mucinous materials?	Yes	Partly no	No
6	The color of the scanned image is even throughout the image?	Yes	Partly no	No
7	The color of the nuclei is even throughout the image?	Yes	Partly no	No
8	The image of overlapping cells or 3-dimensional clusters is clear enough to interpret?	Yes	Partly no	No
9	Is it easy to differentiate nuclei and cytoplasm of the cells (especially in the overlapping clusters)?	Yes	Partly no	No
10	The cytoplasmic membrane is clear enough to interpret?	Yes	Partly no	No
11	The nuclear membrane is clear enough to interpret?	Yes	Partly no	No
12	Is the image good enough to assess the cytoplasmic texture?	Yes	Partly no	No
13	Is the image good enough to assess the nuclear chromatin pattern?	Yes	Partly no	No
14	Is the image good enough to assess the nucleoli?	Yes	Partly no	No
15	Is the image good enough to assess the necrosis (only apply when the case includes necrosis)?	Yes	Partly no	No
16	Is the focus clear enough in the higher magnification?	Yes	Partly no	No
17	Is the focus clear enough in the lower magnification?	Yes	Partly no	No

clarity of the cytoplasmic and nuclear membranes, ability to assess the texture and chromatin pattern, and presence of necrosis in the image. Finally, questions addressed the clarity of the image at higher and lower magnifications. For each question, the quality was rated as 1 (yes/all), 2 (partially no, <10%), or 3 (no, >10%).

## RESULTS

### Parallel digital pathology and glass PTs and post-test feedback survey

In 2020, 216 institutes participated in conventional PT, and 48 institutes participated in trial digital PT as a supplementary test for the third and fourth programs. In 2021, 215 institutes, including 85 university hospitals, 80 general hospitals, and 45 commercial laboratories, participated in PT, 108 institutes par-

ticipated in digital PT, and 107 institutes participated in conventional glass-slide PT. The glass slides for conventional PT were collected 2 years prior to PT as a fourth program. In 2022, 211 institutes, including 85 university hospitals, 80 general hospitals, and 45 commercial laboratories, participated in PT, 81 institutes participated in digital PT, and 130 institutes participated in conventional glass-slide PT. The concordance rates of digital and conventional PT based on various sample types are summarized in Fig. 1.

In 2020, the overall concordance rates were 77.6% for the digital PT and 81.9% for the conventional PT using glass slides (Fig. 1A). The concordance rates were not significantly different in thyroid fine-needle aspiration (FNA) (digital vs. conventional PT, 94.3% vs. 93.8%) and other FNA samples (87.5% vs. 85.0%), whereas they were significantly lower in the digital PT

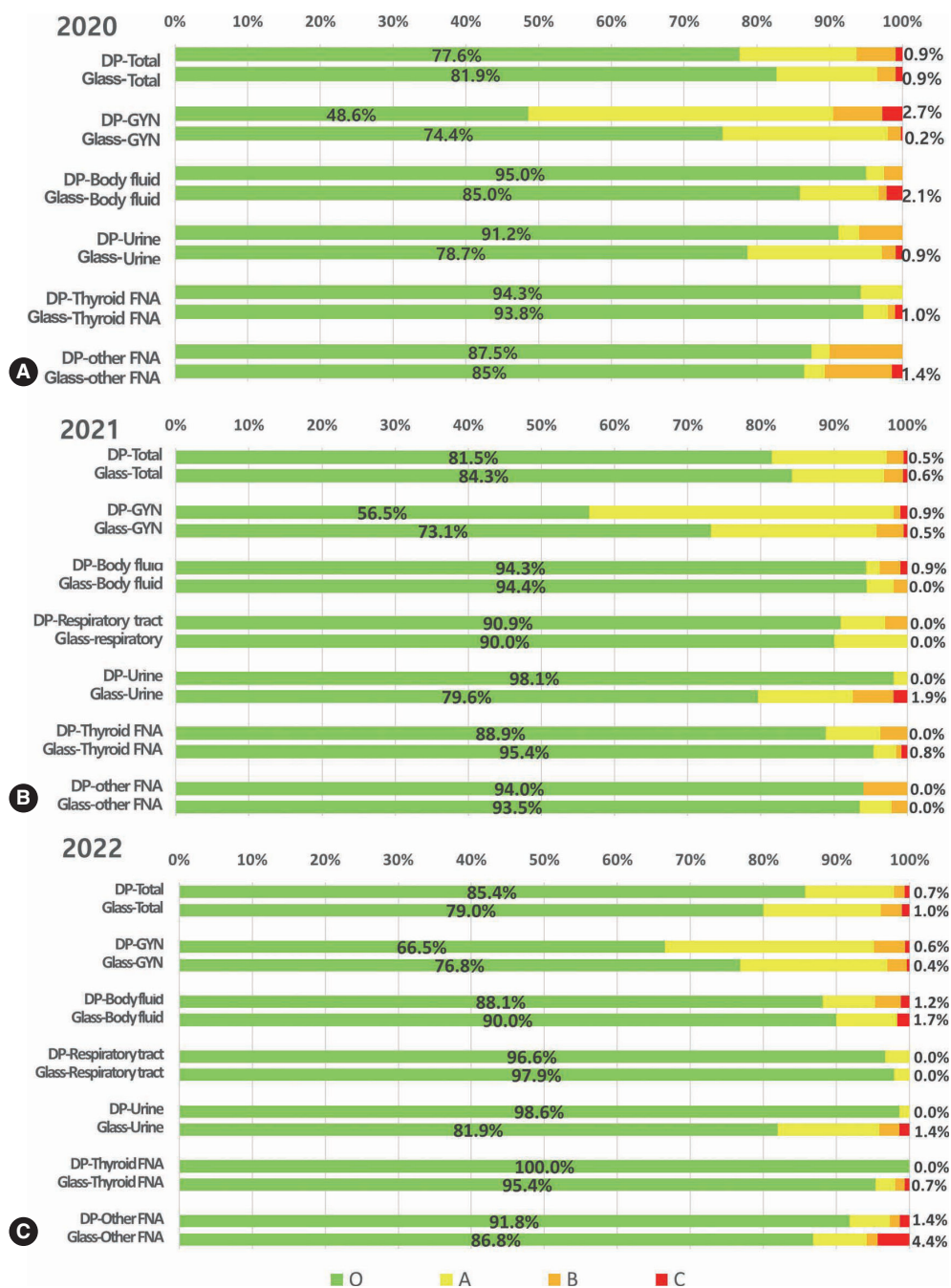


**Fig. 1.** Concordance rate of digital pathology (DP) and glass proficiency tests in 2020 (A), 2021 (B), and 2022 (C). O, concordancy; A, minimal discordancy; B, minor discordancy; C, major discordancy. GYN, gynecologic samples; FNA, fine-needle aspiration.

of gynecologic samples (48.6% vs. 74.4%) and significantly higher in the digital PT of body fluid (95.0% vs. 85.0%) and urine samples (91.2% vs. 78.7%) (Fig. 1A). More cases of minor and minimal discordance exist in digital PT than in conventional PT. The number of cases with major discordance affecting clinical practice was similar, less than 1% for both digital and glass PT (0.9%).

In 2021, the overall concordance rates were 81.5% for digital PT and 84.3% for conventional PT using glass slides (Fig. 1B). The concordance rates were not significantly different in body fluid samples (digital vs. conventional, 94.3% vs. 94.4%), respiratory tract samples (90.9% vs. 90.0%), and other FNA samples (94.0% vs. 93.5%), while they were moderately lower in digital PT of gynecologic samples (56.5% vs. 73.1%) and thyroid

FNA (88.9% vs. 95.4%) and significantly higher in digital PT of urine samples (98.1% vs. 79.6%) (Fig. 1B). Cases with minor discordance were more common in digital PT, whereas cases with minimal discordance were similar in both digital and conventional PT. The cases with major discordance were similar, with <1% in both digital and glass PT (0.9%).

In 2022, the overall concordance rates were 85.4% for digital PT and 79.0% for conventional PT using glass slides (Fig. 1C). The concordance rates were not significantly different in body fluid samples (digital vs. conventional, 88.1 vs. 90.0%) and respiratory tract samples (96.6% vs. 97.9%), while they were moderately lower in digital PT of gynecologic samples (66.5% vs. 76.8%), and significantly higher in digital PT of urine (98.6% vs. 81.9%), thyroid FNA (100.0% vs. 95.4%), and other FNA samples (91.8% vs. 86.8%) (Fig. 1C). Cases with minor and minimal discordance were more in conventional PT, and cases with major discordance were similar, with <1% in both digital and glass PT (0.7% vs. 1.0%).

Significant changes were noted in the results over time in that the concordant cases of digital PT significantly increased every year, showing better concordance than conventional PT in 2022. The cases with minor and minimal discordance in digital PT significantly reduced than conventional PT over time, although the cases with major discordance were relatively similar every year. Regarding the sample types, only cases with minimal discordance were more frequent in gynecologic samples in digital PT than in conventional PT in 2022. These results indicate that participants gradually became familiar with digital platforms in most sample types, yet room for progress remains in gynecologic samples, where diagnostic categories are complex and highly segmented.

Fig. 2 summarizes the post-test feedback survey after digital PT in 2020, 2021, and 2022. All participants (48 institutes for digital PT and 168 institutes for conventional PT in 2020, 107 for digital PT and 108 for conventional PT in 2021, and 82 for digital PT and 133 for conventional PT in 2022) submitted ratings for the given slides/image quality (Fig. 2A, E, I). In 2020, 79.7% of the respondents said that the quality of the digital images was good, whereas only 69.1% said that the conventional slides were of good quality (Fig. 2A). In 2021, 72.7% and 71.5% of the respondents reported good-quality digital images and conventional slides, respectively (Fig. 2E). In 2022, 73.7% and 71.5% of the respondents reported good-quality digital images and conventional slides, respectively (Fig. 2I). In 2020, the percentage of respondents who reported bad quality of slides/images was slightly higher in the conventional PT group than in the digital group by 3.7% vs. 1.6%, although these numbers were

slightly higher in the digital group than in the conventional group in 2021 (5.6% vs. 2.6%) and 2022 (4.3% vs. 3.0%). The respondents who reported good slide/image quality were similar or slightly higher in the digital group than in the conventional group for all 3 years. In 2020, nine out of 48 institutes that participated in digital PT as a supplementary test responded to the survey, while 76 out of 107 institutes responded to the survey after participation in digital PT in 2021, and 19 out of 82 institutes responded to the survey after participation in digital PT in 2022 (Fig. 2B–D, 2F–H, 2J–L). The majority of the respondents reported generally good or very good image, service quality, or satisfactory levels by sample type in 2020, and similar results were found in 2021 and 2022 except for a very limited number of respondents reporting bad or slightly bad image, service quality, or satisfactory levels by sample type in 2021 as the number of gross participants increased (Fig. 2B–D, 2F–H, 2J–L).

### Comparative assessment of whole slide images of cytologic samples according to scanners

#### General product specification according to scanners

The product specifications of the five digital scanners are listed in Table 3. The Panoramic 250 Flash of 3DHitech offers a high-speed slide scanning with a maximum resolution of 0.23  $\mu\text{m}/\text{pixel}$ , making it an ideal choice for high-throughput laboratories. The Panoramic 250 flash scanner had a slide capacity of 250 and a scan speed of 3 minutes for a 5  $\times$  5-mm-sized slide at 40 $\times$  magnification with five layers of z-stacking. It has an excellent graphical user interface and produces an excellent image quality at 40 $\times$  magnification. The file size of a 15  $\times$  15-mm-sized slide at 40 $\times$  magnification with five layers of z-stacking is 10 GB. The scanner has a weekly capacity of 200 slides and can operate in the bright-field and fluorescent imaging modes. It supports MRXS, JPG, and JPG2000 digital slide formats and has a multilayer support system with either a Z-stack or an extended focus. The error rate per run is 2 and has a special feature of continuous loading.

Conversely, the NanoZoomer 360 of Hamamatsu has a fast-scanning speed with a maximum resolution of 0.23  $\mu\text{m}/\text{pixel}$  and allows multiple users to access the system simultaneously. It has a slide capacity of 360 and a scan speed of 1.5 min for a 5  $\times$  5-mm-sized slide at 40 $\times$  magnification with five layers of z-stacking. It has a good GUI and produces good image quality at 40 $\times$  magnification. The file size of a 15  $\times$  15-mm-sized slide at 40 $\times$  magnification with five layers of z-stacking is 10 GB. The scanner has a weekly capacity of 300 slides and can operate in the



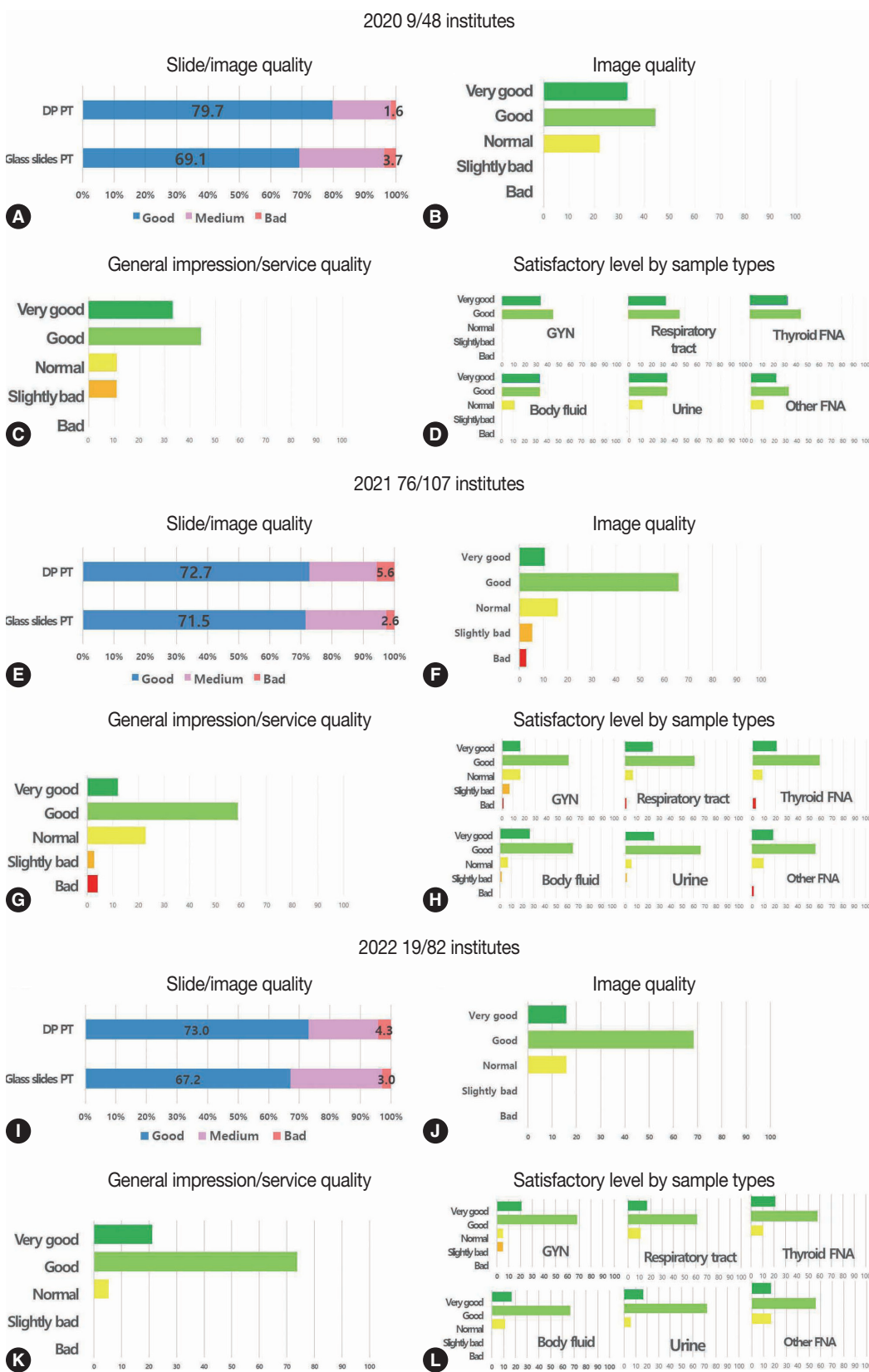


**Fig. 2.** Post-test feedback survey after digital pathology (DP) proficiency test (PT) in 2020 (A-D), 2021 (E-H), and 2022 (I-L). GYN, gynecologic samples; FNA, fine-needle aspiration.

**Table 3.** Product specification of whole slide scanners included in this study

Manufacturer	3DHistech	Hamamatsu	Leica	Roche	Philips
Model	Pannoramic 250 Flash	NanoZoomer 360	Aperio AT2	Ventana DP 200	Ultra-Fast Scanner
Slide capacity	250	360	400	6	300
Scan speed 5 × 5 mm (40×) – 5 layers	3 min	1.5 min	2.5 min	1.5 min	-
GUI (user friendliness)	Excellent	Good	Satisfactory	Satisfactory	-
Image quality (40×)	Excellent	Good	Excellent	Good	-
File size 15 × 15 mm (40×) 5 layers	10 GB	10 GB	8 GB	12 GB	-
Magnification	20×, 40×	20×, 40×	20×, 40×	20×, 40×	20×, 40×
Weekly capacity (slides)	200	300	150	< 100	-
Imaging mode(s)	Bright field, fluorescent	Bright field	Bright field, fluorescent	Bright field	Bright field
Digital slide format	MRXS, JPG, and JPG2000	JPG, ndpi	TIFF (SVS)	BIF	Insyntax, fic
Multilayer support	Z-stack or extended focus	Z-stack or extended focus	Z-stack	Extended focus	Not support
Error rate <sup>a</sup>	2	3	4	3	-
Special features	Continuous loading	Quality scoring and intelligent rescans	Automated scanning	-	LCD touchscreen

GUI, graphical user interface.

<sup>a</sup>Error rate per run.

bright-field imaging mode. It supports the JPG and NDPI digital slide formats and has a multilayer support system with either a Z-stack or an extended focus. The error rate per run was 3, and it has special features of quality scoring and intelligent rescans.

The Leica Aperio AT2 scanner had a slide capacity of 400 and a scan speed of 2.5 min for a 5 × 5-mm-sized slide at 40× magnification with five layers of z-stacking. It has a satisfactory GUI and produces an excellent image quality at 40× magnification. The file size of a 15 × 15-mm-sized slide at 40× magnification with five layers of z-stacking is 8 GB. The scanner has a weekly capacity of 150 slides and can operate in the bright-field and fluorescent imaging modes. It supports the TIFF (SVS) digital slide format and has a multilayer support system with a Z-stack. The error rate is 4 per run and has a special feature of automated scanning.

The Roche Ventana DP200 is a fully automated slide scanner that can scan up to 200 slides simultaneously with a maximum resolution of 0.25 μm/pixel. It has a slide capacity of 6 and a scan speed of 1.5 min for a 5 × 5-mm-sized slide at 40× magnification with five layers of z-stacking. It has a satisfactory GUI and produces good image quality at 40× magnification. The file size of a 15 × 15 mm-sized slide at 40× magnification with five layers of z-stacking is 12 GB. The scanner has a weekly capacity of less than 100 slides and can operate in the bright-field imaging mode. It supports the BIF digital slide format and has a multilayer support system with an extended focus. The error rate for each run was 3.

Philips' Ultra-Fast Scanner has a unique dual-camera system

that allows the scanning of both bright-field and fluorescent slides with a maximum resolution of 0.25 μm/pixel. The slide capacity is 300, and the scan speed is extraordinarily fast for general HE-stained tissue slides but does not provide z-stacking because it was originally not targeting cytologic samples. As a result, it generally produces suboptimal image quality for cytological samples at 40× magnification. It supports only the bright-field imaging mode, syntax and fic digital slide formats. No information was provided on the weekly capacity or error rate.

#### Scanning area coverage according to scanners

A difference in the scanning area coverage was noted between the whole slide scanners (WSSs), and a representative case example is shown in Fig. 3. The Panoramic Flash 250 III of 3DHistech showed the largest coverage in general, AT2, NanoZoomer S360, and Ventana DP200 showed similar coverage, while the Ultra-Fast Scanner by Philips showed the smallest scanning area coverage. Scanning coverage is directly related to scanning time and file size. The larger the scanning coverage, the longer the scanning time, and the larger the file size. In other words, as the Panoramic Flash 250 III covers the largest scanning area, it takes the longest scanning time and generates the largest file size, whereas the Ultra-Fast Scanner takes the shortest scanning time and generates the smallest file size because it covers the smallest scanning area. The difference in scanning coverage did not appear to be very effective for proper or impaired diagnosis in the included cases, although concluding that the coverage represents the eligibility for proper diagnosis and the integrity of digital slide



Fig. 3. Difference in scanning area coverage between whole-slide scanners in representative cases.

images is not possible.

#### Qualitative analysis of the image quality of the scanned images

Figs. 4 to 6 show the differences between the scanned images of representative samples. In general, color differences exist in terms of contrast, temperature, hue, saturation, sharpness, brightness, exposure, clarity, and background based on the WSSs. This may be a subjective matter that varies among individuals. It should also be noted that the color can be adjusted or optimized using different color subsets or profiles within the viewer program and monitor settings. The color of the WSIs scanned by 3DHistech tends to show more vivid images with a slightly exaggerated contrast. We can see orangophilic squamous cells in the pap smear of squamous intraepithelial lesion more eminently in the WSIs scanned by 3DHistech (Fig. 4A, B). The color of the WSIs scanned using the Roche WSS was slightly higher than that of the green tint. The WSIs scanned using Philips presented realistic colors, although the images were fuzzy and less clear than the others. The background of the WSIs was the brightest among the 3DHistech WSIs. Fig. 5 shows the differences between the scanned images of representative body fluid samples, squamous cell carcinoma of the lungs on a conventional bronchial washing smear (Fig. 5A), metastatic adenocarcinoma on a conventional pleural fluid smear (Fig. 5B), serous carcinoma on a conventional ascitic fluid smear (Fig. 5C), and high-grade non-invasive papillary urothelial carcinoma on a urine cytology sample (Fig. 5D) scanned using three Z-stacking layers. Fig. 6 shows the difference in scanned images of FNA samples including pleomorphic adenoma of salivary gland on conventional smear

with three layers of z-stacking (Fig. 6A), and metastatic ductal carcinoma of lymph node on a conventional smear scanned with three layers of z-stacking (Fig. 6B). The images present different image qualities and characteristics according to the scanners in terms of nuclei and nucleoli features, three-dimensional clusters, and singly dispersed cells, as the scanners provide different technical specifications (see also Supplementary Fig. S2 for the rest of the samples).

#### Image quality assessment using a questionnaire by experienced cytopathologists

Fig. 7 shows the overall average results of the image quality assessment using a questionnaire administered by four experienced cytopathologists. The number in each cell represents the average rating and is marked as a color spectrum from green for 1 (yes/all) to red for 3 (no/>10%). As we can see in the figure, the cells are more likely to be red in DP200 (Roche) and Ultra-Fast Scanner (Philips), which are originally not designed for cytology and do not support z-stacking. The differences between the Flash 250 III by 3DHistech, Aperio AT2 by Leica, and NanoZoomer 360 by Hamamatsu were generally not significant, although the Flash 250 III by 3DHistech showed the best satisfactory results in most of the questionnaires.

## DISCUSSION

The results of the digital and glass PT were found to be comparable in 2021 and 2022. Feedback from participating institutes was generally positive for the DP PT. The 3DHistech Pannoram-

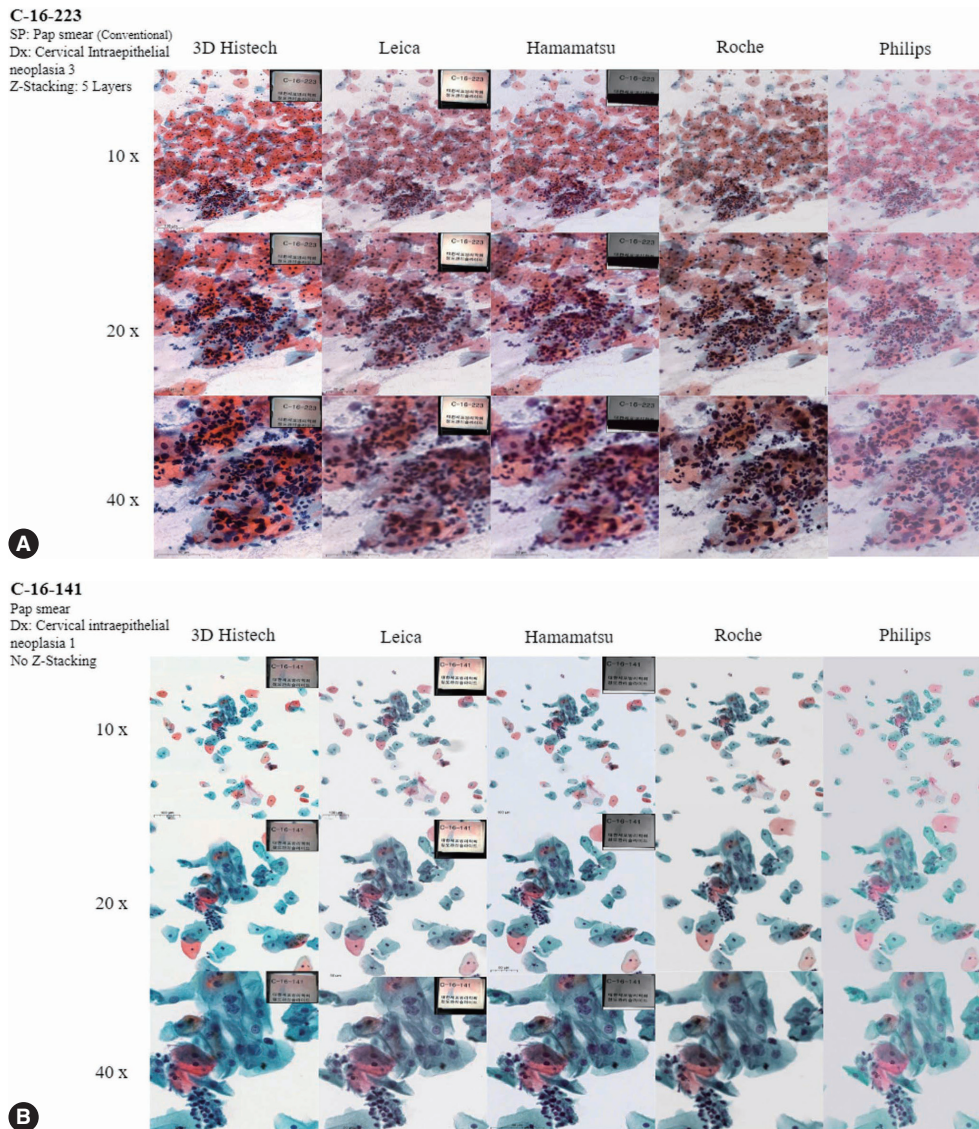


**Fig. 4.** Difference in scanned images of a few representative gynecologic samples (Pap smear). (A) High squamous intraepithelial lesion on a conventional Pap smear scanned with five layers of z-stacking. (B) Low squamous intraepithelial lesion on a liquid-based preparation scanned without z-stacking.

ic 250 Flash III showed generally satisfactory image quality with high capacity, featuring large coverage, even focus, good z-stacking features, low error rates, and continuous loading [11]. The device had the highest contrast and strongest saturation but resulted in a longer scanning time and larger file size. Conversely, the Leica AT2 showed generally satisfactory image quality with high capacity, offering middle coverage with sharp and well-focused images, good z-stacking features, and high compatibility. However, it had a slightly dark hue, slightly outdated user interface and usability, longer scanning time, and slightly higher error rate.

The Hamamatsu NanoZoomer S360 generally showed satis-

factory image quality with high capacity, featuring acceptable coverage, good scanning speed, even focus, good z-stacking features, and appropriate color and saturation [12]. Despite having the smallest file size, it remains in the process of registration with the KFDA. The Roche Ventana DP200 also demonstrated generally satisfactory image quality, but with limited capacity, offering good coverage, good focus with extended z-stacking, good color, and specialization for companion diagnosis and image analysis [13]. However, its capacity is limited, although with a good scanning speed. The Philips Intellisite Ultra-Fast Scanner has good image quality, but poor focus for 3D-cluster-rich samples [14]. The device had good speed and capacity, and the most real-

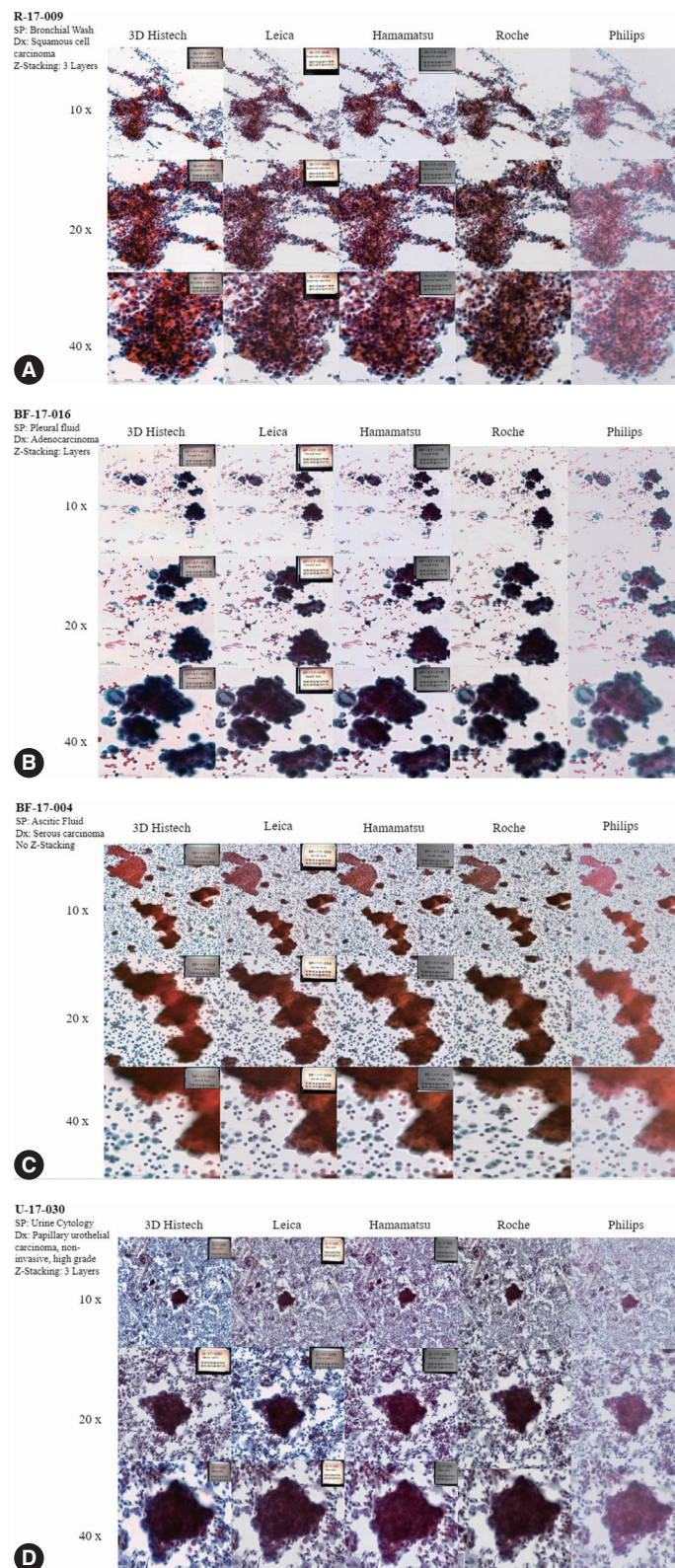


**Fig. 5.** Difference in the scanned images of a few representative body fluid samples. (A) Squamous cell carcinoma of the lungs on a conventional bronchial washing smear scanned with three layers of z-stacking. (B) Metastatic adenocarcinoma on a conventional pleural fluid smear scanned with three layers of z-stacking. (C) Serous carcinoma on a conventional ascitic fluid smear scanned without z-stacking. (D) Non-invasive papillary urothelial carcinoma, high grade, on a urine cytology sample scanned with three layers of z-stacking.

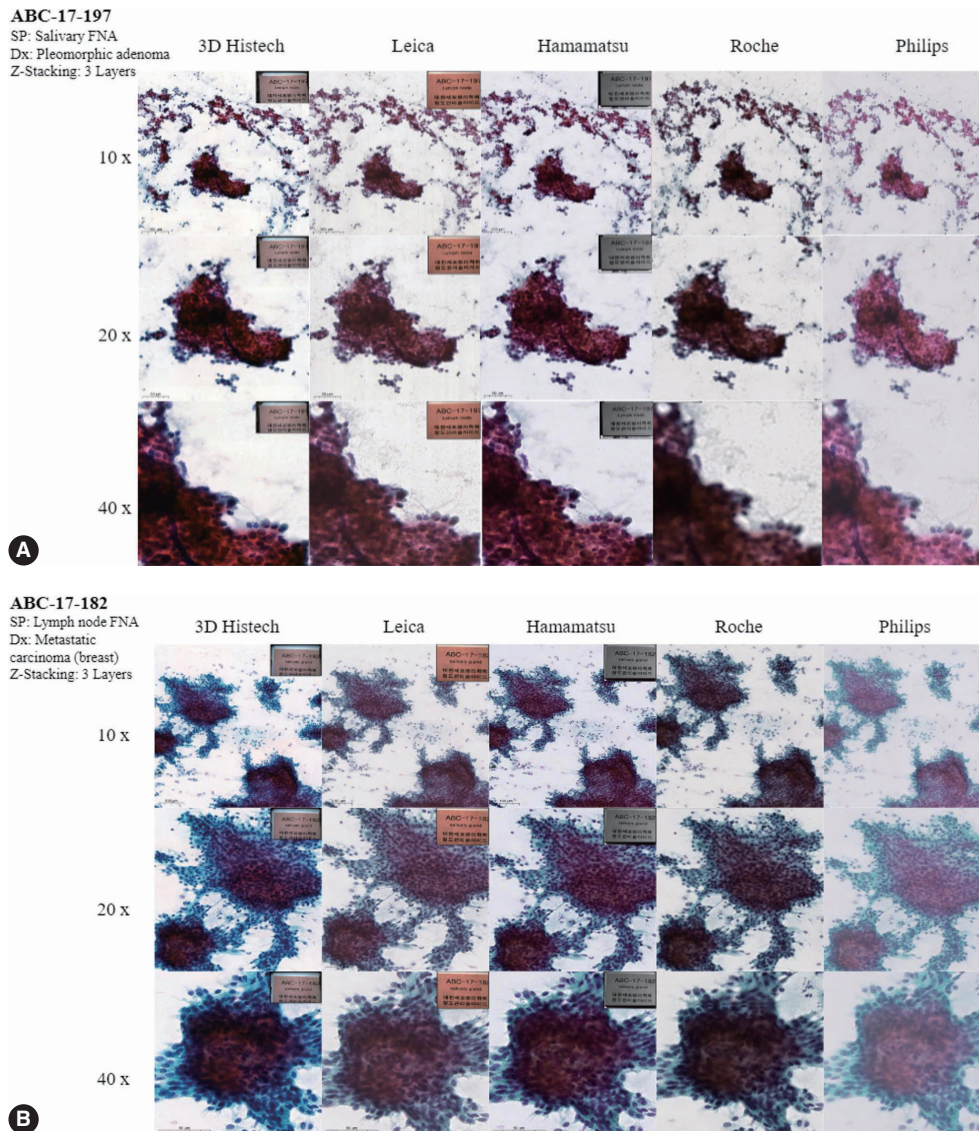


**Fig. 6.** Difference in scanned images of a few representative fine-needle aspiration cytology samples. (A) Pleomorphic adenoma of salivary gland on conventional smear scanned with three layers of z-stacking and (B) metastatic ductal carcinoma of lymph node on a conventional smear scanned with three layers of z-stacking.

istic hue, color, saturation, and contrast, but poor coverage and poor focus owing to the lack of z-stacking (good image quality in GYN LBP), a slightly high error rate, and limited compatibility.

To date, evidence for the validity of DP application in cytological samples is insufficient. This is mainly because of the requirement of a higher resolution such as 100× for cytologic samples that can demonstrate good visibility for nuclear-level features, such as chromatin patterns and nucleolar features, the so-called image quality. Another main reason that pathologists use DPS for cytology is the longer scanning time, larger file size of digital cytological images, and higher error rates, which can be a burden for managing and storing systems as well as image analysis

processes.

At the 2023 Annual Meeting of the United States of America and Canadian Association of Pathologists, Akbar et al. presented a poster at Ohio State University Wexner Medical Center [15]. In this study, the authors compared the technical performance of four WSI scanners, including the Ultra-Fast Scanner by Philips, AT2 and GT450 by Leica, and the Genius Digital Diagnostics System by Hologic, on 250 cytology slides with different preparations [15]. The overall successful scan rate ranges from 38% to 96%, with the Hologic scanner showing the best performance and ThinPrep slides showing the highest success rate [15]. The fail-to-scan rates remained significant, indicating

Questions		3DHistech Flash250III	Leica Aperio AT2	Hamamatsu NanoZoomer 360	Roche DP200	Philips UltraFast Scanner
1	All the area of the slide were scanned properly?	1.2	1.4	1.5	1.5	1.5
2	The scanned image show even magnification in all the area?	1.3	1.6	1.7	1.7	1.6
3	The white balance of the backgroud image are appropriate?	1	1.3	1.2	1.4	1.4
4	Is the focus of the image even enough throughout the image?	1.4	1.7	1.8	1.9	2.2
5	Is it easy to differentiate cells and background artifacts such as inflammatory cells and mucinous materials?	1.1	1.4	1.4	1.6	1.7
6	The color of the scanned image is even throughout the image?	1.1	1.3	1.4	1.4	1.4
7	The color of the nuclei is even throughout the image?	1.1	1.4	1.4	1.4	1.4
8	The image of overlapping cells or 3-dimensional clusters is clear enough to interpret?	1.6	1.8	1.9	2.1	2.2
9	Is it easy to differentiate nuceli and cytoplasm of the cells (especially in the overlapping clusters)?	1.4	1.8	1.9	2	2.1
10	The cytoplasmic membrane is clear enough to interpret?	1.2	1.4	1.6	1.6	1.7
11	The nuclear membrane is clear enough to interpret?	1.2	1.4	1.6	1.7	1.8
12	Is the image good enough to assess the cytoplasmic texture?	1.2	1.4	1.7	1.7	1.9
13	Is the image good enough to assess the nuclear chromatin pattern?	1.2	1.4	1.6	1.9	2
14	Is the image good enough to assess the nucleoli?	1.3	1.5	1.8	1.9	2
15	Is the image good enough to assess the necrosis (only apply when the case include necrosis)?	1	1.7	1.7	1.7	1.7
16	Is the focus clear enough in the higher magnification?	1.6	1.8	1.9	2	2.2
17	Is the focus clear enough in the lower magnification?	1.2	1.3	1.3	1.5	1.6

Fig. 7. Result of image quality assessment using a questionnaire by four experienced cytopathologists.

that a digital cytology workflow for primary diagnosis is currently infeasible. Further experience and evidence should be provided for the safe implementation of digital cytology.

Recently, Hologic launched a new scanner system for cytologic specimens, along with an artificial intelligence (AI) algorithm for gynecologic samples, called Genius Digital Diagnostics [16], which is a pioneering digital cytology platform that has obtained CE-mark certification through integrating advanced volumetric imaging technology with a novel AI algorithm to assist cyto-technologists and pathologists in detecting precancerous lesions and cancer cells in women. The platform can swiftly examine every cell on a ThinPrep Pap digital image, reducing tens of thousands of cells to an AI-curated gallery showing the most diagnostically significant images [16,17]. This system provides an AI algorithm for gynecologic samples and its API is planned to open to third-party applications to expand its coverage to AI algorithms for non-gynecologic samples, such as urine, body fluids, and FNAs.

Currently, one of the major challenges in applying AI to cytology is the significantly larger size of cytologic whole-slide images compared with histology [18,19]. This not only leads to a more time-consuming scanning process but also demands increased computational resources for image analysis. This was largely due to the Z-stacking process, which is essential for cytological samples [18,20]. In addition, the image quality can vary depending on the scanner used, which can affect the effectiveness of AI algorithms. Another challenge in cytology is the difficulty of annotating images, particularly when dealing with image patches or cell clusters. Furthermore, the limited availability of well-annotated large datasets, publicly accessible datasets, and significant challenges can hinder the development and testing of AI models

[21–24]. Volumetric scanning technology, which was recently introduced by the Genius Digital Diagnostics system, can be a good solution to these issues by scanning slides tangentially at once and combining the acquired images into a single layer of images by post-processing computation. This allows fast scanning with an optimal focus resulting in a much smaller file size.

Unfortunately, the latest systems, including Genius Digital Diagnostics by Hologic and GT450 by Leica, were not included in this study because they were not publicly released at the time of the study design. Several new scanners, such as Optrascan, Morphle, and Olympus, have been developed and introduced by traditional and new companies. Further studies comparing scanners from various vendors are required. In addition, it should also be clearly understood that the DP200 by Roche and the Ultra-Fast Scanner by Philips were not originally intended to be applied for cytological samples, but for histological samples.

Based on the analysis of different scanner models, having at least three layers of z-stacking is recommended for LBP and five layers of z-stacking for conventional smears to achieve optimal image quality. The selection of a scanner model should be based on careful consideration of the institutional characteristics of the cytopathology practices. To ensure the best fit in practice, a thorough test run of the candidate scanner models is recommended.

Digital scanners are essential tools in modern pathology laboratories. They provide high-resolution digital images of the tissue samples that can be easily viewed, stored, and shared electronically. The aim of this study was to compare the product specifications and image quality of cytologic slides scanned using five digital scanners: Panoramic 250 Flash of 3DHistech, NanoZoomer 360 of Hamamatsu, Aperio AT2 of Leica, Ventana DP200 of Roche, and Ultra-Fast Scanner of Philips. In conclu-

sion, each digital scanner has strengths and limitations. The Panoramic 250 Flash of 3DHitech and NanoZoomer 360 (Hamamatsu) are best suited for high-throughput laboratories, whereas the Aperio AT2 (Leica) and Ventana DP200 (Roche) are best suited for the high-resolution scanning of a large number of slides. Philips' Ultra-Fast Scanner is an excellent choice for laboratories that require both bright-field and fluorescence imaging. Therefore, the selection of an appropriate digital scanner depends on specific laboratory requirements.

### Supplementary Information

The Data Supplement is available with this article at <https://doi.org/10.4132/jptm.2023.07.17>.

### Ethics Statement

This study was reviewed and approved by the Institutional Review Board of the Catholic University of Korea College of Medicine (UC21ZCSI0133). The informed consent was waived by the Institutional Review Board of the Catholic University of Korea College of Medicine.

### Availability of Data and Material

Data and materials for this work are available from the corresponding author upon reasonable request.

### Code Availability

Not applicable.

### ORCID

Yosep Chong <https://orcid.org/0000-0001-8615-3064>  
 Soon Auck Hong <https://orcid.org/0000-0002-7902-4608>  
 Hoon Kyu Oh <https://orcid.org/0000-0001-8793-1948>  
 Soo Jin Jung <https://orcid.org/0000-0002-9139-701X>  
 Bo-Sung Kim <https://orcid.org/0000-0002-2344-7230>  
 Ji Yun Jeong <https://orcid.org/0000-0001-6167-4998>  
 Ho-Chang Lee <https://orcid.org/0000-0003-4687-8348>  
 Gyungyub Gong <https://orcid.org/0000-0001-5743-0712>

### Author Contributions

Conceptualization: YC, SAH, HKO, SJJ, BSK, JYJ, GG. Data curation: YC, SAH, HKO, SJJ, BSK. Formal analysis: YC. Funding acquisition: YC, GG. Investigation: YC, SAH, HKO, SJJ, BSK, JYJ. Methodology: YC, SAH, HKO, SJJ, BSK, JYJ. Project administration: YC, SAH. Resources: SAH, HKO, SJJ, BSK, JYJ. Software: YC. Supervision: GG, HCL.

### Conflicts of Interest

Y.C., a contributing editor of the *Journal of Pathology and Translational Medicine*, was not involved in the editorial evaluation or decision to publish this article. All remaining authors have declared no conflicts of interest.

### Funding Statement

This study was partially supported by a Korean Society for Cytopathology grant (No. 2019-01) and a National Research Foundation of Korea (NRF) grant funded by the Korean government (MSIT) (No. 2021R1A2C2013630).

### Acknowledgments

I thank Mr. Muhammad Joan Ailia, Dr. Jamshid Abdul-Ghafar, and Dr.

Mohammad Rizwan Alam for data curation and manuscript styling.

### References

- Lee HK, Kim SN, Khang SK, Kang CS, Yoon HK. Quality control program and its results of Korean Society for Cytopathologists. *Korean J Cytopathol* 2008; 19: 65-71.
- The Korean Society for Cytopathology [Internet]. Seoul: The Korean Society for Cytopathology, 2023 [cited 2023 Apr 25]. Available from: <http://eng.cytopathol.or.kr/index.asp>.
- Oh EJ, Jung CK, Kim DH, et al. Current cytology practices in Korea: a nationwide survey by the Korean Society for Cytopathology. *J Pathol Transl Med* 2017; 51: 579-87.
- Chong Y, Bae JM, Kang DW, Kim G, Han HS. Development of quality assurance program for digital pathology by the Korean Society of Pathologists. *J Pathol Transl Med* 2022; 56: 370-82.
- Hong SA, Jung H, Kim SS, et al. Current status of cytopathology practice in Korea: impact of the coronavirus pandemic on cytopathology practice. *J Pathol Transl Med* 2022; 56: 361-9.
- Chong Y, Jung H, Pyo JS, Hong SW, Oh HK. Current status of cytopathology practices in Korea: annual report on the Continuous Quality Improvement program of the Korean Society for Cytopathology for 2018. *J Pathol Transl Med* 2020; 54: 318-31.
- Choi YD, Oh HK, Kim SJ, et al. Continuous quality improvement program and its results of Korean Society for Cytopathology. *J Pathol Transl Med* 2020; 54: 246-52.
- Chong Y, Kim DC, Jung CK, et al. Recommendations for pathologic practice using digital pathology: consensus report of the Korean Society of Pathologists. *J Pathol Transl Med* 2020; 54: 437-52.
- The Royal College of Pathologist of Australasia Quality Assurance Programs (RCPAQAP) [Internet]. St. Leonards: The Royal College of Pathologist of Australasia, 2023 [cited 2023 Apr 15]. Available from: <https://rcpaqap.com.au/about-us/>.
- UK National External Quality Assessment Service (NEQAS) [Internet]. Sheffield: UK NEQAS, 2023 [cited 2023 Apr 25]. Available from: <https://ukneqas.org.uk/about-us/>.
- Pannoramic 250 Flash Series Digital Scanners [Internet]. Budapest: 3DHISTECH, 2023 [cited 2023 Apr 26]. Available from: <https://www.3dhitech.com/research/pannорamic-digital-slide-scanners/pannорamic-250-flash-iii/>.
- Nano Zoomer S360 Digital slide scanner [Internet]. Hamamatsu: HAMAMATSU Photonics K.K., 2023 [cited 2023 Apr 26]. Available from: <https://www.hamamatsu.com/us/en/product/life-science-and-medical-systems/digital-slide-scanner/C13220-01.html/>.
- VENTANA DP 200 slide scanner [Internet]. Rotkreuz: F Hoffmann-La Roche Ltd., 2023 [cited 2023 Apr 26]. Available from: <https://diagnostics.roche.com/global/en/products/instruments/ventana-dp-200-ins-6320.html>.
- Ultra Fast Scanner [Internet]. Amsterdam: Philips Intellisite, 2023 [cited 2023 Apr 26]. Available from: <https://www.usa.philips.com/healthcare/product/HCNOCN442/ultra-fast-scanner-digital-pathology-slide-scanner/>.
- Akbar S, Sinclair D, Shen R, Parwani AV, Li Z. Comparative assessment of digital scanners for scanning cytology slides. In: USCAP Annual Meeting; 2023 Mar 11-16; New Orleans, LA.
- Genius Digital Diagnostics System [Internet]. Marlborough: HOLOGIC, 2023 [cited 2023 Apr 25]. Available from: <https://www.hologic.com/hologic-products/cytology/genius-digital-diagnostics-system/>.



17. Yao K, Sadimin E, Chang S, Schmolze D, Li Z. Current applications and challenges of digital pathology in cytopathology. *Hum Pathol Rep* 2022; 28: 300634.
18. Capitanio A, Dina RE, Treanor D. Digital cytology: a short review of technical and methodological approaches and applications. *Cytopathology* 2018; 29: 317-25.
19. Niazi MK, Parwani AV, Gurcan MN. Digital pathology and artificial intelligence. *Lancet Oncol* 2019; 20: e253-61.
20. Hanna MG, Monaco SE, Cuda J, Xing J, Ahmed I, Pantanowitz L. Comparison of glass slides and various digital-slide modalities for cytopathology screening and interpretation. *Cancer Cytopathol* 2017; 125: 701-9.
21. Xu C, Li M, Li G, Zhang Y, Sun C, Bai N. Cervical cell/clumps detection in cytology images using transfer learning. *Diagnostics (Basel)* 2022; 12: 2477.
22. Hipp JD, Sica J, McKenna B, et al. The need for the pathology community to sponsor a whole slide imaging repository with technical guidance from the pathology informatics community. *J Pathol Inform* 2011; 2: 31.
23. Hartman DJ, Van Der Laak J, Gurcan MN, Pantanowitz L. Value of public challenges for the development of pathology deep learning algorithms. *J Pathol Inform* 2020; 11: 7.
24. Thakur N, Alam MR, Abdul-Ghafar J, Chong Y. Recent application of artificial intelligence in non-gynecological cancer cytopathology: a systematic review. *Cancers (Basel)* 2022; 14: 3529.

# Establishing molecular pathology curriculum for pathology trainees and continued medical education: a collaborative work from the Molecular Pathology Study Group of the Korean Society of Pathologists

Jiwon Koh<sup>1</sup>, Ha Young Park<sup>2</sup>, Jeong Mo Bae<sup>1</sup>, Jun Kang<sup>3</sup>, Uiju Cho<sup>4</sup>, Seung Eun Lee<sup>5</sup>, Haeyoun Kang<sup>6</sup>,  
 Min Eui Hong<sup>7</sup>, Jae Kyung Won<sup>1</sup>, Youn-La Choi<sup>8</sup>, Wan-Seop Kim<sup>5</sup>, Ahwon Lee<sup>3,9</sup>,  
 The Molecular Pathology Study Group of the Korean Society of Pathologists

<sup>1</sup>Department of Pathology, Seoul National University Hospital, Seoul National University College of Medicine, Seoul;

<sup>2</sup>Department of Pathology, Busan Paik Hospital, Inje University College of Medicine, Busan;

<sup>3</sup>Department of Hospital Pathology, Seoul St. Mary's Hospital, College of Medicine, The Catholic University of Korea, Seoul;

<sup>4</sup>Department of Pathology, St. Vincent's Hospital, College of Medicine, The Catholic University of Korea, Suwon;

<sup>5</sup>Department of Pathology, Konkuk University Medical Center, Konkuk University School of Medicine, Seoul;

<sup>6</sup>Department of Pathology, CHA Bundang Medical Center, CHA University, Seongnam;

<sup>7</sup>Department of Pathology, Chung-Ang University Hospital, Seoul;

<sup>8</sup>Department of Pathology and Translational Genomics, Samsung Medical Center, Sungkyunkwan University School of Medicine, Seoul;

<sup>9</sup>Cancer Research Institute, College of Medicine, The Catholic University of Korea, Seoul, Korea

**Background:** The importance of molecular pathology tests has increased during the last decade, and there is a great need for efficient training of molecular pathology for pathology trainees and as continued medical education. **Methods:** The Molecular Pathology Study Group of the Korean Society of Pathologists appointed a task force composed of experienced molecular pathologists to develop a refined educational curriculum of molecular pathology. A 3-day online educational session was held based on the newly established structure of learning objectives; the audience were asked to score their understanding of 22 selected learning objectives before and after the session to assess the effect of structured education. **Results:** The structured objectives and goals of molecular pathology was established and posted as a web-based interface which can serve as a knowledge bank of molecular pathology. A total of 201 pathologists participated in the educational session. For all 22 learning objectives, the scores of self-reported understanding increased after educational session by 9.9 points on average (range, 6.6 to 17.0). The most effectively improved items were objectives from next-generation sequencing (NGS) section: 'NGS library preparation and quality control' (score increased from 51.8 to 68.8), 'NGS interpretation of variants and reference database' (score increased from 54.1 to 68.0), and 'whole genome, whole exome, and targeted gene sequencing' (score increased from 58.2 to 71.2). Qualitative responses regarding the adequacy of refined educational curriculum were collected, where favorable comments dominated. **Conclusions:** Approach toward the education of molecular pathology was refined, which would greatly benefit the future trainees.

**Key Words:** Molecular pathology; Training; Residents

**Received:** August 3, 2023 **Revised:** August 20, 2023 **Accepted:** August 26, 2023

**Corresponding Author:** Ahwon Lee, MD, Department of Hospital Pathology, College of Medicine, The Catholic University of Korea, Seoul St. Mary's Hospital, 222 Banpo-daero, Seocho-gu, Seoul 06591, Korea  
 Tel: +82-2-2258-1621, Fax: +82-2-2258-1627, E-mail: klee@catholic.ac.kr

Molecular pathology (MP) refers to various diagnostic techniques based on the handling of nucleic acids [1]. The area of MP has been increasing in both its amount and importance since the introduction of targeted therapy and integrated molecular pathology diagnosis [2-4]. Especially after the introduction of clinical next-generation sequencing (NGS), the importance of MP for

practicing pathologists is continuously growing [5]. In South Korea, the clinical NGS has become a part of daily practice since 2017, and the test volumes have increased, and currently in the year 2023, a total of 69 institutions in Korea is performing clinical NGS tests [6]. In the year 2021, 15,842 NGS tests were performed nationwide according to the statistics obtained from the

Big Data Hub of Korean Health Insurance Review & Assessment Service [6]. Therefore, there is a great need for efficient training of MP for pathology trainees and as continued medical education (CME).

In United States, the Association for Molecular Pathology Training and Education Committee presented general goals and objectives for MP education in residency program in 1999 [7]. In Korea, general goals and objectives for pathology residency training is demonstrated by Ministry of Health and Welfare [8], which includes the statements regarding specialized tests including MP techniques; however, well organized and structured educational curriculum is still insufficient and not well established yet.

Unlike in United States, practicing MP in Korea has some unique features; for instance, (1) departments of clinical pathology and anatomic pathology are separated, (2) MP testings and reimbursements are controlled under unique governmental regulations, and (3) some of the genetic features of Korean population is different from the Western data. Thus, customized MP educational curriculum well suited for the Korean practicing environment should be developed for adequate training of Korean pathology residence and CME.

To develop a refined educational curriculum of MP, the Molecular Pathology Study Group of the Korean Society of Pathologists (KSP) appointed a task force (TF) composed of experienced molecular pathologists, structured objectives and goals of MP and posted as a web-based interface, provided 3-day online structured MP educational session, and received immediate feedbacks from the trainees and practicing pathologists.

## MATERIALS AND METHODS

The Molecular Pathology Study Group of the KSP appointed a TF composed of experienced molecular pathologists to develop a refined educational curriculum of MP. The TF initially started with literature review of MP education and training approaches in US and established structured key learning objectives of MP training in Korea. Online resource repository composed of key references for each learning objective was organized by the TF.

Based on the newly established structure of learning objectives, 3-day online MP educational sessions were held on February 2, 12, and 26, 2022. To assess the usefulness of the learning objective-oriented educational sessions, the TF also created survey asking the session audience to score their understanding of selected learning objectives before and after the session by Likert scale.

## RESULTS

### Lessons from US experiences

In US, the need for adequate MP education started around late 1990s [9], owing to the advances in the application of molecular biology technology. In the year 1999, the Training and Education Committee of Association for Molecular Pathology (AMP) provides an outline of important elements of resident MP education [7]. The general goals provided by the AMP include basic knowledge in human genetics, basics of molecular biology, and specific skills relevant to microbiology, molecular oncology, genetics, histocompatibility, and identity determination [7]. In addition, the AMP also provided the list of sentinel papers highlighting the important concepts of infectious disease, molecular oncology, inherited disorders, histocompatibility, and identity determination [7].

Along with the advances in NGS technologies and increase in the importance of genomic medicine in the clinical practice, the need for the refinement of educational topics was increased over time. Therefore, the Stanford group pioneered to establish a genomic pathology curriculum—so-called The Stanford Open Curriculum—to help pathology residents build a foundation for the understanding of genomic medicine and the implications for clinical practice [10]. The 10 lectures encompassed the overview of the fundamental principles of molecular biology, clinical genomics, and personalized medicine, and the curriculum also provided 7 additional topics as the elective course of advanced genomic medicine [11].

However, the real-world data suggested that there existed a significant discrepancy between the literal description of curriculum and the subjective perception among the trainees. In a survey of 42 pathology residency programs, only 31% reported that genomic medicine training was included in their program [12]. The serious educational gap prompted the pathologists and medical education specialists in US to organize Training Residents in Genomics (TRIG) Working Group. The TRIG Working Group conducted a nationwide survey for the in-serviced pathology residents in 2013 [13]. 42% and 7% of residents reported that they had no training of genomic medicine and MP during their residency, respectively [13]. When asked whether they were able to discuss MP or genomic medicine test results with a provider, only 13% and 28% of the responders scored that their ability as “very good/excellent” [13].

On observing the obvious educational gap, the Training and Educational Committee of AMP appointed the Molecular Curriculum Task Force; the TF developed an organized curriculum

**Table 1.** Structured goals and objectives of molecular pathology training

1	Gene and genome
1-1	Able to explain the composition and structure of DNA and RNA
1-2	Able to explain the definition of genome, exome, proteome, transcriptome, and metabolome
1-3	Able to explain the chromosome, histone, and chromatin
1-4	Able to explain the replication and repair process of DNA
1-5	Able to explain the mechanism and regulator of transcription
1-6	Able to explain the mechanism of translation and definition of codons
1-7	Able to explain the definition of promoter, enhancer, cis- and trans-regulation
1-8	Able to explain the types and roles of epigenetic gene regulation
1-9	Able to explain the definition of genetic polymorphism
1-10	Able to explain the definition of point mutation, insertion, deletion, and structural variation including translocation
1-11	Able to explain the definition of missense, synonymous, nonsense, null, and frameshift mutations
1-12	Able to explain the association between mutations and genomic instability and RNA splicing
2	Molecular oncology (introduction)
2-1	Able to explain the definition of oncogene and tumor suppressor gene
2-2	Able to explain the hallmark of cancer
2-3	Able to explain the major cellular signaling pathways related to oncogenesis and cancer progression
2-4	Able to explain the mechanism through which proto-oncogenes are activated and transformed into oncogenes
2-5	Able to explain the mechanisms of familial and hereditary tumor development
2-6	Able to explain the definition of chromosomal instability and loss of heterozygosity
2-7	Able to explain the definition and clinical significance of mismatch repair deficiency, microsatellite instability, homologous recombination deficiency, tumor mutational burden
2-8	Able to explain the definition and clinical significance of methylation in cancer
2-9	Able to list the indications of molecular pathology testings in cancer (i.e., screening, diagnostic, prognostic, predictive, treatment monitoring)
2-10	Able to explain the definitions of companion diagnostics and complementary diagnostics
2-11	Able to list the predictive markers of major cancer types
3	Techniques of molecular pathology
3-1	Able to explain the DNA/RNA extraction process according to the sample types
3-2	Able to explain the ways of assessing quality and quantity of DNA/RNA and list the pros and cons of each method
3-3	Able to list the ways of assessing genetic mutations and list the pros and cons of each method
3-4	Able to explain why the minimum tumor requirement differs between assays
3-5	Able to explain the factors influencing the quality of tissue samples and nucleic acid
3-6	Able to properly name the genetic mutations according to the Human Genome Variation Society (HGVS) nomenclature
3-7	Able to explain the assessment process and criteria of the clinical performance evaluation
3-8	Able to explain the assessment process and criteria of the analytical performance evaluation
4	Sanger sequencing
4-1	Able to explain the principle of Sanger sequencing and interpretation
4-2	Able to interpretate the electropherogram of each type of mutation
4-3	Able to identify the causes of false positive or false negative results
4-4	Able to interpretate the mutation analysis results and generate proper clinical reports
4-5	Able to list the specific disease-related genetic mutations
5	Next-generation sequencing (NGS)
5-1	Able to explain the differences between NGS and Sanger sequencing
5-2	Able to explain the differences between hybrid capture and amplicon-based target enrichment
5-3	Able to explain the definitions of whole genome, whole exome, targeted gene panel, and transcriptome sequencing and pros/cons of each method
5-4	Able to explain each step of library preparation for NGS
5-5	Able to explain each step of bioinformatic analysis for NGS data
5-6	Able to explain the major quality metrics related to the qualities of library and sequencing data
5-7	Able to list major reference database for use in variant interpretation and definition of tier-based classification system
6	Polymerase chain reaction (PCR)
6-1	Able to explain the principle and indication of PCR
6-2	Able to list the technical considerations of performing PCR
6-3	Able to interpretate the PCR analysis results and generate proper clinical reports
6-4	Able to explain the principle and indication of real-time PCR (RT-PCR)

*(Continued to the next page)*

**Table 1.** Continued

6-5	Able to list the technical considerations of performing RT-PCR
6-6	Able to interpretate the RT-PCR analysis results and generate proper clinical reports
7	In situ hybridization (ISH)
7-1	Able to explain the principle and process of fluorescent in situ hybridization (FISH), chromogenic in situ hybridization (CISH), and silver in situ hybridization (SISH)
7-2	Able to list the indications of FISH, CISH, and SISH
7-3	Able to explain the types of FISH probes
7-4	Able to explain the clinical significance of FISH results
7-5	Able to interpretate the results of FISH, CISH, SISH and generate proper clinical reports
8	Microsatellite instability (MSI) test
8-1	Able to explain the definition of microsatellite
8-2	Able to explain the principles and techniques of MSI tests
8-3	Able to explain the clinicopathological significance of MSI
9	Methylation analysis
9-1	Able to explain the principles and techniques of methylation analysis
9-2	Able to explain the definition of CpG island methylator phenotype
9-3	Able to list the technical considerations of performing methylation analysis
9-4	Able to interpretate the results of methylation analysis and generate proper clinical reports
10	Gene rearrangement test
10-1	Able to explain the definition of gene rearrangement and utilize the results in the diagnosis and treatment planning
10-2	Able to list the methods of gene rearrangement tests and explain the pros/cons of each method
10-3	Able to interpretate the results of gene rearrangement analysis and generate proper clinical reports
11	Human papillomavirus genotyping by DNA microarray
11-1	Able to explain the principle of DNA microarray and utilize the results in the diagnosis and treatment planning
11-2	Able to explain the process of DNA microarray test
11-3	Able to list the methods of DNA microarray tests and explain the pros/cons of each method
11-4	Able to interpretate the results of DNA microarray analysis and generate proper clinical reports
12	Chromosome analysis
12-1	Able to explain the principle of chromosome analysis
12-2	Able to explain the result and clinical significance of chromosome analysis
13	Molecular pathology laboratory management
13-1	Able to list precautions for preventing cross-contamination during each step of molecular pathology testings
13-2	Able to list the reference database for genetic testings
13-3	Able to list the credential criteria and quality metrics for laboratory certificate
13-4	Able to guide the clinicians for proper molecular pathology testings
13-5	Able to explain the definitions of research use only, investigational use only, in vitro diagnostics, laboratory developed test, and analyte specific reagents

MMR, mismatch repair; MSI, microsatellite instability; HRD, Homologous recombination deficiency; TMB, tumor mutation burden; NGS, next-generation sequencing; PCR, polymerase chain reaction; FISH, fluorescent in situ hybridization; CISH, chromogenic in situ hybridization; SISH, silver in situ hybridization.

in MP for residents [14]. The major subjects of curriculum included basic MP goals/laboratory management, basic concepts in molecular biology and genetics, technology, inherited disorders, oncology, infectious diseases, pharmacogenetics, histocompatibility and identity, genomics, and information management [14]. Besides, TRIG Working Group provided online genomic pathology modules to improve genomics knowledge and the ability to utilize online genomics tools (<https://www.pathology-learning.org/trig>). The first version was introduced in the year 2016, and the most recent updates were added in the year 2020 [15,16]. To date, the TRIG has expanded their work toward the education of the undergraduate medical students [17].

### Learning objectives and online repository

For adaptation of US experiences into real-world education in South Korea, 13 major topics of MP education was selected by the TF, and detailed description of objectives and goals were generated under each topic, comprising a total of 75 structured items as shown in Table 1. The structured objectives included basic items such as ‘1-2. *Definition of genome, exome, proteome, transcriptome, and metabolome*’, and further encompassed timely topics such as ‘2-10. *Able to explain the definitions of companion diagnostics and complementary diagnostics.*’

To provide high-quality resources for trainees, TF members were assigned with each major topic and reviewed the relevant

online resources and assessed the quality of contents. After the thorough review of contents, the most adequate learning sources were selected and gathered to form the online repository of MP learning objectives. The online repository became available for all the members of KSP via the official webpage ([https://www.pathology.or.kr/html/?pmode=boardlist&MMC\\_pid=306&cate=study](https://www.pathology.or.kr/html/?pmode=boardlist&MMC_pid=306&cate=study)) (Fig. 1).

### 3-Day online structured educational session and survey

Based on the structural objectives, the Molecular Pathology Study Group of the KSP planned and held 3-day online structured educational session in February 2022 (Table 2). A total of 201 pathologists participated in the educational session.

To immediately assess the effectiveness of refined educational session, the TF selected 22 key learning objectives out of total 75 elements and asked the session audience to grade their understanding of each topic before and after the lecture, respectively. The survey was performed at day 1 and day 2 with response rates as follows: day 1 pre-lecture, 93/201 (46.3%); day 1 post-lecture 83/201 (41.3%); day 2 pre-lecture 50/201 (24.9%); day 2 post-

lecture 34/201 (16.9%).

Among 22 learning objectives (Fig. 2), the audience reported higher scores regarding their prior understanding on the basic concepts of MP including '1-1. Composition and structure of DNA and RNA' (mean score 72.8), '2-1. Oncogene and tumor suppressor gene' (mean score 73.0), and '6-1. Principle and indication of PCR' (mean score 73.5). In contrast, self-reported understanding prior to the session was lowest in the topics related to NGS: '5-6. Quality metrics of NGS library and sequencing data' (mean score 51.8); '5-7. Database for variant interpretation' (mean score 54.1); '5-3. Whole genome, whole exome, target gene, and transcriptome sequencing' (mean score 58.2).

The scores of self-reported understandings increased after educational session by 9.9 points on average (range, 6.6 to 17.0) (Fig. 2). Of interest, the most effectively improved items were those with lowest pre-lecture scores as follows: '5-6. Quality metrics of NGS library and sequencing data' (score increased from 51.8 to 68.8); '5-7. Database for variant interpretation' (score increased from 54.1 to 68.0); '5-3. Whole genome, whole exome, target gene, and transcriptome sequencing' (score increased from 58.2 to 71.2).

The screenshot displays the website of the Korean Society of Pathologists (KSP). The main content area lists learning objectives, such as '4. 분자병리 방법론 (각론) - Sanger 염기서열법' and '5. 분자병리 방법론 (각론) - 차세대 염기서열법'. A detailed view of objective 5-1 is shown, listing several sub-objectives related to NGS methods and data analysis. Each sub-objective includes a 'Resource link' button. A zoomed-in view of a resource link is shown in the bottom right panel, displaying the title 'Guidelines for Validation of Next-Generation Sequencing-Based Oncology Panels' and the URL <https://doi.org/10.1016/j.jmoldx.2017.01.011>.

**Fig. 1.** Snapshot showing the online repository of structured molecular pathology goals and learning objectives. The repository of learning objectives became available online for all the members of Korean Society of Pathologists. Each element is linked with high-quality learning resources as shown in the bottom right panel.

**Table 2.** The course overview of 3-day molecular pathology educational session

Day 1	
1	Introduction to molecular pathology
2	DNA/RNA
3	Gene expression
4	Epigenetics
5	Molecular oncology (I)
6	Molecular oncology (II)
7	Hallmark of cancer
Day 2	
1	Molecular technology (1) – Principle, application, and practice
2	Molecular technology (2) – Principle, application, and practice
3	Molecular technology (3) – Principle, application, and practice
4	NGS system: Technology & wet-lab
5	NGS-bioinformatics and knowledge base
6	NGS interpretation and reporting: in the view of pathologists
7	Pathologists role in immuno-oncology
8	Companion diagnosis/liquid biopsy
Day 3	
1	Molecular diagnostics & personalized medicine in breast
2	Molecular diagnostics & personalized medicine in female genital tract
3	Molecular diagnostics & personalized medicine in gastrointestinal tract
4	Molecular diagnostics & personalized medicine in primary brain tumor
5	Molecular diagnostics & personalized medicine in endocrine organ
6	Molecular diagnostics & personalized medicine in urogenital tract
7	Molecular diagnostics & personalized medicine in lung and mediastinum
8	Molecular diagnostics & personalized medicine in skin
9	Molecular diagnostics & personalized medicine in hematopathology
10	Molecular diagnostics & personalized medicine in bone and soft tissue

Additionally qualitative responses regarding the adequacy of refined educational curriculum were collected, where favorable comments dominated. The audience provided responses regarding the further suggestions regarding the topic for future educational sessions, and some of the examples are as follows: real-world clinical NGS cases, NGS raw data analysis using R software, wet-lab techniques of NGS, and cutting-edge novel technologies including proteomics and proteogenomics.

## DISCUSSION

In line with the recent increase in need for the high-quality education of MP for pathology trainees, the Molecular Pathology Study Group of the KSP initiated this project for the development of MP curriculum.

The project first started with the review of US experiences on the MP education during the last decade [7,9-12,14-18]. Next, the project focused on the establishment of the structured objec-

tives and goals of MP, which was later online resource repository within KSP official website to enable continuous update and better accessibility. Also, 3-day structured course was held according to the newly established learning objectives, which received favorable responses from the audience.

The TF appointed by the Molecular Pathology Study Group of the KSP specifically aimed to list up learning objectives and goals, which can readily be introduced into practical educational sessions, like the successful experience by TRIG Working Group [12,16,17]. These efforts resulted in the production of online resource repository and 3-day online MP course. The favorable responses from the KSP members suggest that the purpose of this project was relatively well achieved. Still, we noticed some limitations and further challenges.

First, unlike the survey performed by TRIG [13], the overall response rate of the survey was low, which implies that the data may not represent the opinions of all the pathology residents in Korea. In addition, our survey did not collect the information with respect to the training levels of audience; since the subjective need for certain items among the learning objectives may differ according to the training level or current job description, further collection of feedbacks from variable groups among KSP members should follow. Moreover, besides the subjective assessment of participants' understandings, well-prepared questionnaires and self-assessment programs for objective measurement of participants' academic accomplishment should be provided in the near future.

The most important challenge that need to be addressed would be the sustainability and timely adaptability of the education curriculum. The area of MP and genomic medicine is one of the most rapidly evolving sectors among the field of pathology [3,4,19]. The efforts from small group of eager pathologists would not be able to maintain the long-lasting high-quality educational platform. Continuous feedback from all the KSP members along with the leadership from Molecular Pathology Study Group of KSP could surely make the quality of MP education better, which would benefit the whole medical society in South Korea. In addition, an in-depth pool of high-quality assessment contents should be further developed for proper evaluation of the educational effect of this novel approach.

In conclusion, for better education of MP within KSP, structured learning objectives and goals of MP was refined and listed, which resulted in the production of online reference repository and 3-day MP lecture course. Approach toward the education of MP was refined, and this big step can further greatly benefit the future trainees.

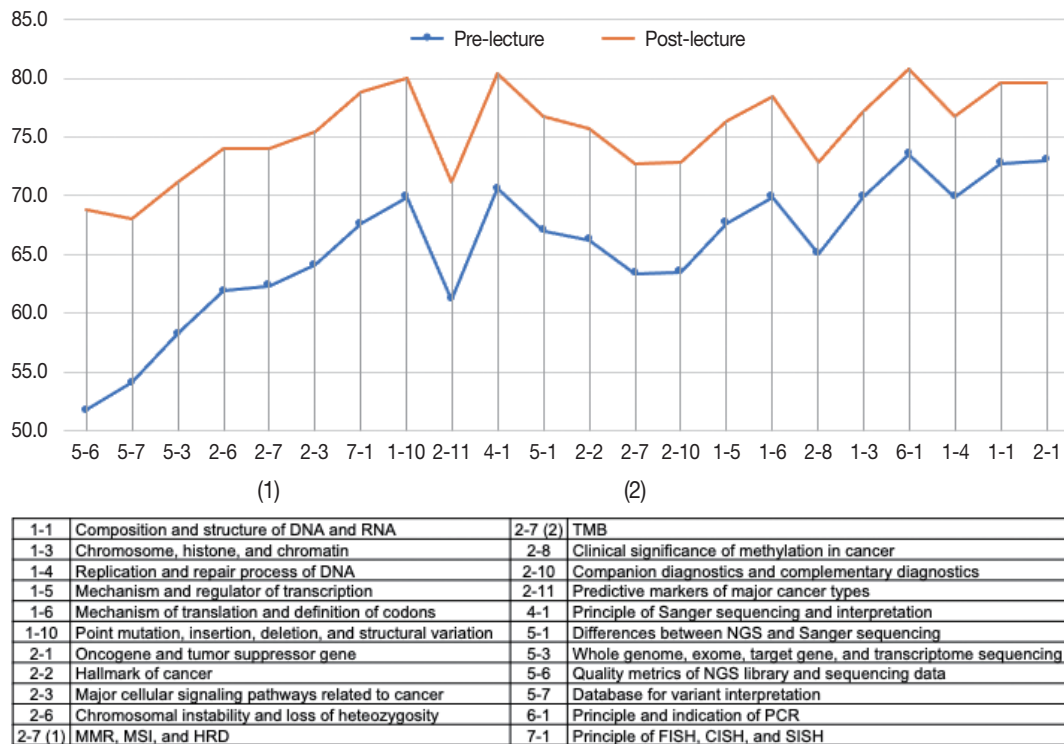


**Fig. 2.** Comparison of subjective understandings on the selected topics between before and after the 3-day structured course. The participants of 3-day structured course were asked to grade their subjective understanding before and after the lecture, and the results for selected topics are depicted.

### Ethics Statement

Not applicable.

### Availability of Data and Material

The datasets used and/or analysed during the current study are available from the corresponding author on reasonable request.

### Code Availability

Not applicable.

### ORCID

Jiwon Koh <https://orcid.org/0000-0002-7687-6477>  
 Ha Young Park <https://orcid.org/0000-0002-7192-2374>  
 Jeongmo Bae <https://orcid.org/0000-0003-0462-3072>  
 Jun Kang <https://orcid.org/0000-0002-7967-0917>  
 Uiju Cho <https://orcid.org/0000-0002-6229-8418>  
 Seung Eun Lee <https://orcid.org/0000-0002-7459-0061>  
 Haeyoun Kang <https://orcid.org/0000-0002-8980-7702>  
 Min Eui Hong <https://orcid.org/0000-0002-4409-4286>  
 Jae Kyung Won <https://orcid.org/0000-0003-1459-8093>  
 Youn-La Choi <https://orcid.org/0000-0002-5788-5140>  
 Wan-Seop Kim <https://orcid.org/0000-0001-7704-5942>  
 Ahwon Lee <https://orcid.org/0000-0002-2523-9531>

### Author Contributions

Conceptualization: AL. Data curation: JK (Jiwon Koh), HYP, UC, JKW, AL. Formal analysis: JK (Jiwon Koh). Funding acquisition: AL. Investiga-

tion: JK (Jiwon Koh), HYP, JKW, AL. Methodology: JK (Jiwon Koh), JKW, AL. Resources: JK (Jiwon Koh), HYP, JMB, JK (Jun Kang), UC, SEL, HK, MEH, JKW, YLC, WSK, AL. Writing—original draft: JK (Jiwon Koh). Writing—review & editing: all authors. Approval of final manuscript: all authors.

### Conflicts of Interest

The authors declare that they have no potential conflicts of interest.

### Funding Statement

This research was supported by The Korean Society of Pathologists Grant No. KSPG2021-02.

### References

- Harris TJ, McCormick F. The molecular pathology of cancer. *Nat Rev Clin Oncol* 2010; 7: 251-65.
- Tobin NP, Foukakis T, De Petris L, Bergh J. The importance of molecular markers for diagnosis and selection of targeted treatments in patients with cancer. *J Intern Med* 2015; 278: 545-70.
- Yoon S, Kim M, Hong YS, et al. Recommendations for the use of next-generation sequencing and the molecular tumor board for patients with advanced cancer: a report from KSMO and KCSG Precision Medicine Networking Group. *Cancer Res Treat* 2022; 54: 1-9.
- Lee SH, Lee B, Shim JH, et al. Landscape of actionable genetic alterations profiled from 1,071 tumor samples in Korean cancer patients. *Cancer Res Treat* 2019; 51: 211-22.
- Kim J, Park WY, Kim NK, et al. Good laboratory standards for



- clinical next-generation sequencing cancer panel tests. *J Pathol Transl Med* 2017; 51: 191-204.
6. Big Data Hub of Korean Health Insurance Review & Assessment Service [Internet]. Wonju: Health Insurance Review & Assessment Service, 2022 [cited 2022 Nov 3]. Available from: <https://opendata.hira.or.kr/>.
  7. The Association for Molecular Pathology Training Education Committee. Goals and objectives for molecular pathology education in residency programs. The Association for Molecular Pathology Training and Education Committee. *J Mol Diagn* 1999; 1: 5-15.
  8. Ministry of Health and Welfare. Residency competency training project [Internet]. Sejong: Introduction of Korean Law Information Center, 2022 [cited 2023 Jun 18]. Available from: <https://www.law.go.kr/>.
  9. Arber DA, Battifora H, Brynes RK, Chang KL, Weiss LM, Wilczynski SP. Certification and training in molecular pathology. *Hum Pathol* 1996; 27: 430-1.
  10. Schrijver I, Natkunam Y, Galli S, Boyd SD. Integration of genomic medicine into pathology residency training: the stanford open curriculum. *J Mol Diagn* 2013; 15: 141-8.
  11. Haspel RL, Genzen JR, Wagner J, Lockwood CM, Fong K; Training Residents in Genomics (TRIG) Working Group. Integration of genomic medicine in pathology resident training. *Am J Clin Pathol* 2020; 154: 784-91.
  12. Haspel RL, Atkinson JB, Barr FG, et al. TRIG on TRACK: educating pathology residents in genomic medicine. *Per Med* 2012; 9: 287-93.
  13. Haspel RL, Rinder HM, Frank KM, et al. The current state of resident training in genomic pathology: a comprehensive analysis using the resident in-service examination. *Am J Clin Pathol* 2014; 142: 445-51.
  14. Aisner DL, Berry A, Dawson DB, Hayden RT, Joseph L, Hill CE. A suggested molecular pathology curriculum for residents: a report of the association for molecular pathology. *J Mol Diagn* 2016; 18: 153-62.
  15. Haspel RL, Ali AM, Huang GC, et al. Teaching genomic pathology: translating team-based learning to a virtual environment using computer-based simulation. *Arch Pathol Lab Med* 2019; 143: 513-7.
  16. Haspel RL, Ali AM, Huang GC. Using a team-based learning approach at national meetings to teach residents genomic pathology. *J Grad Med Educ* 2016; 8: 80-4.
  17. Wilcox RL, Adem PV, Afshinnekoo E, et al. The Undergraduate Training in Genomics (UTRIG) Initiative: early & active training for physicians in the genomic medicine era. *Per Med* 2018; 15: 199-208.
  18. Clay MR, Fisher KE. Bioinformatics education in pathology training: current scope and future direction. *Cancer Inform* 2017; 16: 1176935117703389.
  19. Zehir A, Benayed R, Shah RH, et al. Mutational landscape of metastatic cancer revealed from prospective clinical sequencing of 10,000 patients. *Nat Med* 2017; 23: 703-13.

# Hepatic small vessel neoplasm: not totally benign, not yet malignant

Madison Miranda, David Howell, Tony El Jabbour

Department of Pathology, Anatomy, and Laboratory Medicine, West Virginia University, Morgantown, WV, USA

Hepatic small vessel neoplasm (HSVN) is a rare vascular tumor with few reports in the literature. While imaging findings may show characteristic enhancement patterns, limited available literature may not reveal the full potential for image-based diagnosis. Histologically, HSVN mimics other entities, though certain morphologic and immunohistochemical findings provide clues for diagnosis. However, HSVN still provides diagnostic challenges, especially on core biopsies with limited material for morphologic and molecular evaluation. While current recommendations are surgical resection and close observation, the long-term course of the tumor is unknown. We report a case of HSVN in a liver with additional feature of organized lymphoid aggregates necessitating additional hematopathology consultation and workup to rule out concurrent entities.

**Key Words:** Hepatic small vessel neoplasm; Liver; Vascular neoplasm

**Received:** May 13, 2023 **Revised:** June 12, 2023 **Accepted:** June 19, 2023

**Corresponding Author:** Tony El Jabbour, MD, Department of Pathology, Anatomy, and Laboratory Medicine, West Virginia University, 64 Medical Center Drive, PO Box 9203, Morgantown, WV 26506-9203, USA

Tel: +1-304-293-3212, Fax: +1-304-293-1627, E-mail: [tony.eljabbour@hsc.wvu.edu](mailto:tony.eljabbour@hsc.wvu.edu)

**Corresponding Author:** Madison Miranda, MD, Department of Pathology, Anatomy, and Laboratory Medicine, West Virginia University, 64 Medical Center Drive, PO Box 9203, Morgantown, WV 26506-9203, USA

Tel: +1-304-293-3212, Fax: +1-304-293-1627, E-mail: [madison.miranda@hsc.wvu.edu](mailto:madison.miranda@hsc.wvu.edu)

Hepatic small vessel neoplasm (HSVN) is a recently described vascular neoplasm of the liver. Morphologically, this tumor is characterized by a mixture of benign and potentially malignant features to include bland cells lining thin-walled vascular channels, low mitotic rate, and infiltrative borders [1]. As these cases are infrequent, radiologic diagnosis is also challenging.

We report a case of liver biopsy with morphologic and immunohistochemical features characteristic of HSVN. Our case was complicated by organized lymphoid aggregates necessitating hematopathology evaluation.

## CASE REPORT

A 63-year-old asymptomatic male with a medical history of hypertension and occasional alcohol use presented for his annual exam. Routine labs demonstrated mildly elevated liver enzymes to include alanine aminotransferase 110 U/L and aspartate aminotransferase 63 U/L. Alkaline phosphatase was normal (50 U/L).

## Radiologic features

An ultrasound demonstrated a 4.7 cm hypochoic lesion in the right lobe of the liver. Liver protocol magnetic resonance imaging (MRI) with intravenous gadolinium-based contrast revealed a well-circumscribed 4.65 cm lesion that was hyperintense on T2 with prompt heterogenous contrast enhancement without washout (Fig. 1). The sonographic appearance and MRI enhancement pattern were not typical for benign lesions, so the patient subsequently underwent image-guided biopsy.

## Morphologic features

The biopsy showed a neoplasm comprised of closely packed, small, thin-walled anastomosing vascular channels lined by bland endothelial cells. The lesion was well-demarcated from adjacent parenchyma, though focally infiltrated into a portal tract. The cells had no significant nuclear atypia or mitotic activity. There was no hobnailing, papillary formation, complex architecture, or necrosis. Background liver showed mild steatosis with no other significant abnormalities. Additionally, there were various-sized aggregates of small lymphoid cells (Fig. 2).

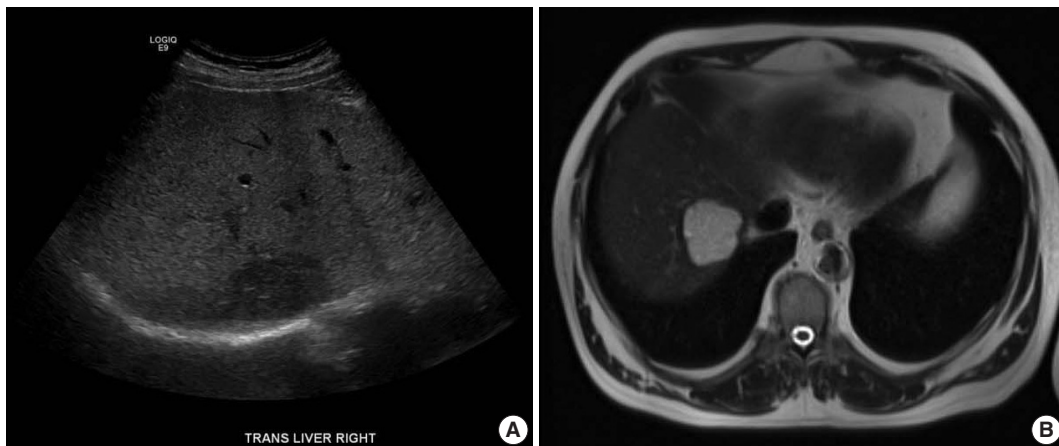


**Fig. 1.** (A) Liver ultrasound demonstrating a hypoechoic lesion in the right lobe of the liver. (B) Liver protocol abdominal magnetic resonance imaging showing a hyperintense lesion on T2 with heterogenous contrast enhancement.

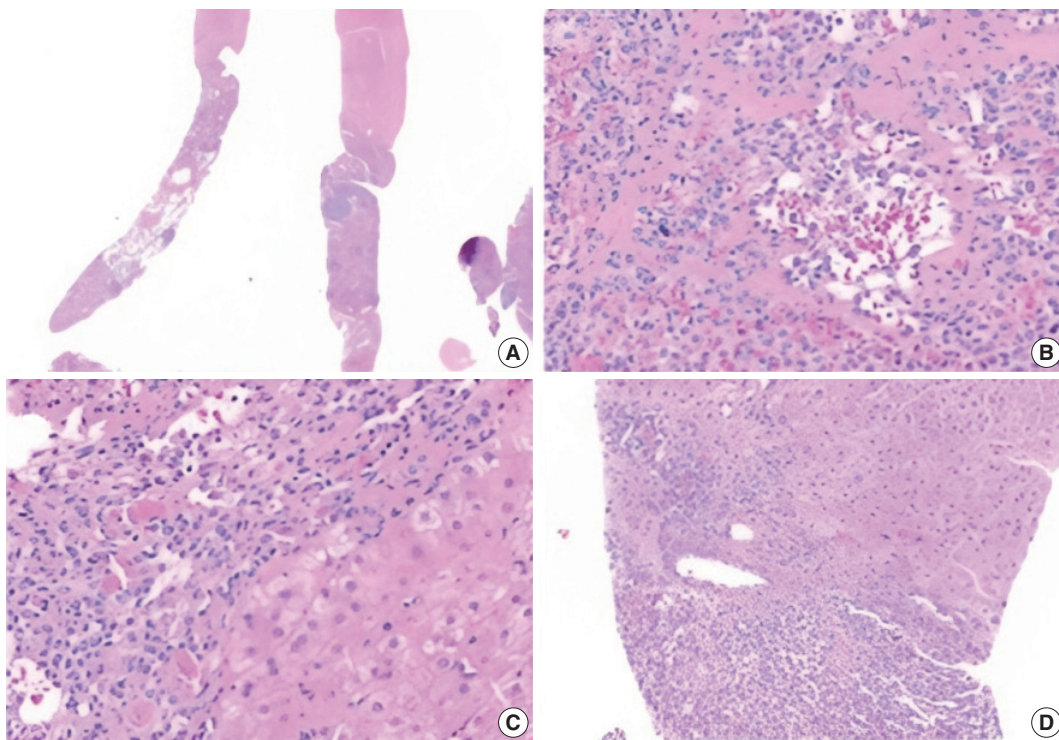


**Fig. 2.** Microscopic appearance of the biopsy specimen. (A) Multiple biopsy specimens with well-demarcated lesion. Multiple, various-sized lymphoid aggregates can be seen. (B) The lesion is composed of thin-walled small vascular channels lined by bland endothelial cells. (C) The lesion is well-demarcated from adjacent liver parenchyma in most areas. (D) Focal infiltration into portal tract.

### Immunohistochemistry

The lesion displayed diffuse positivity for vascular markers (CD34, CD31, and ERG). p53 was patchy/weak (wild type). Neoplastic cells showed Ki-67 proliferation index of 5%–10% (Fig. 3). Iron, Periodic Acid-Schiff with diastase, and copper stains were negative in the background liver.

Additional work-up was completed to exclude ectopic spleen

and/or lymphoma. CD3 and CD20 immunostains highlight mixtures of mature T cells and B cells, respectively, with a predominance of the former. CD8 stains a subset of the T cells, and no splenic sinusoidal endothelial cells are present. These findings exclude ectopic splenosis and are not compatible with a B-cell lymphoma (Fig. 4).

Morphologic and immunohistochemical findings were con-

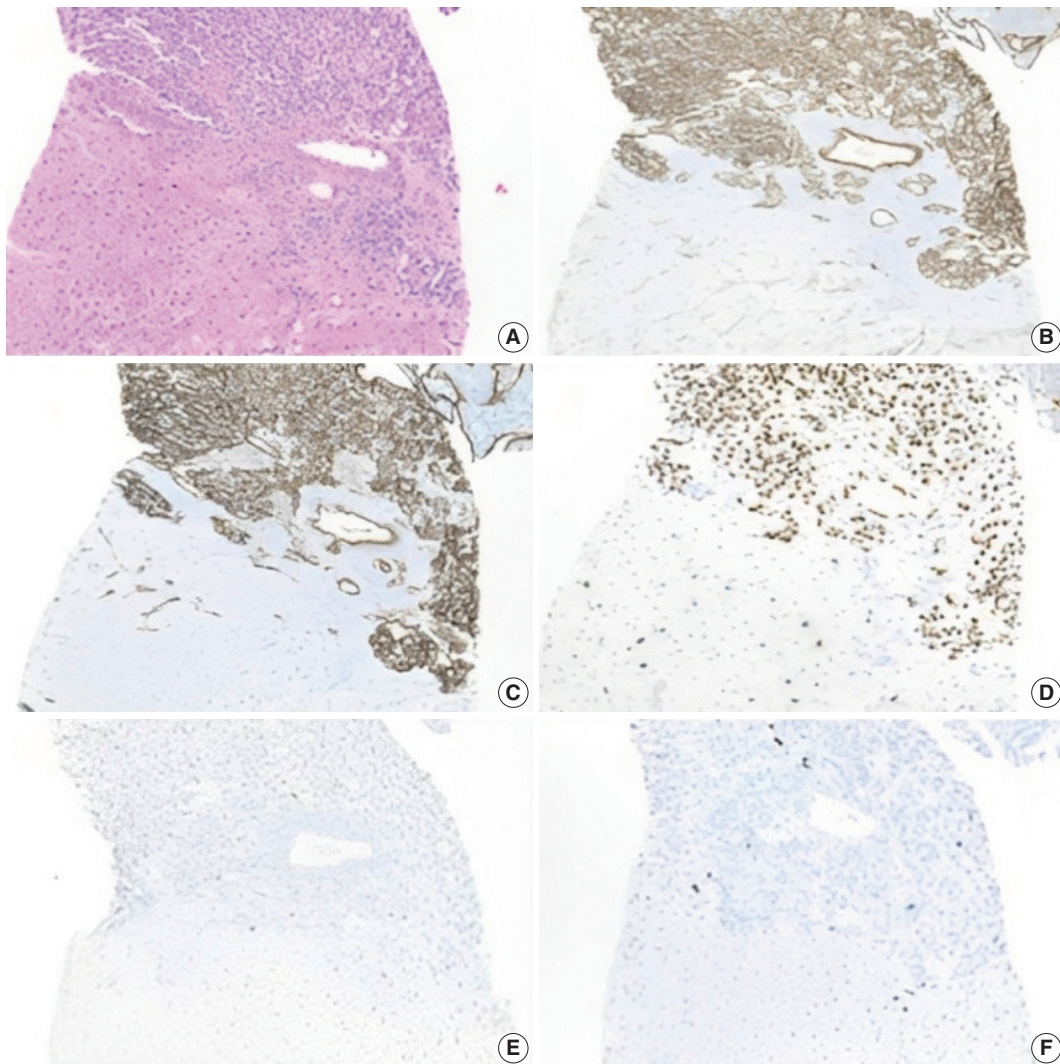


**Fig. 3.** Immunohistochemical staining. (A) Lesion next to normal hepatic parenchyma. (B) The lesion is positive for CD31. (C) Positive for CD34. (D) Positive for ERG. (E) p53 is patchy and weak. (F) Ki-67 proliferation index is 5%–10%.

sistent with HSVN. Though most of the biopsy specimen showed a well-demarcated neoplasm, focal infiltration into a portal tract favored this diagnosis. The case was sent to an expert with special interest in HSVN, who agreed with our assessment [1].

#### Follow-up

The patient was seen by the hepatobiliary surgical team. Treatment options were discussed, including surgical resection, yttrium radioembolization, or observation with serial imaging. The patient opted for observation.

### DISCUSSION

HSVN is a rare vascular neoplasm of the liver with morpho-

logic features that make diagnosis challenging. HSVN is usually incidentally found, and ranges in size from 0.2 to 16 cm [1-3]. It is characterized by strong expression of vascular markers (CD31, CD34, FLI-1, and ERG) and is pancytokeratin negative. All cases have a low Ki-67 proliferation index (<10%) [4]. Next-generation sequencing has shown activating hotspot mutations in the alpha subfamily of G-proteins (*GNAQ*, *GNA11*, and *GNA14*) [5]. In one particular case, foci of high-grade transformation were noticed microscopically while *RAF1* and *GNA11* concurrent mutations were detected at the molecular level. A link between these unique morphology and molecular profile was hypothesized [6].

Anastomosing hemangioma (AH), another rare vascular neoplasm, was at the top of our differential diagnosis list. It is char-

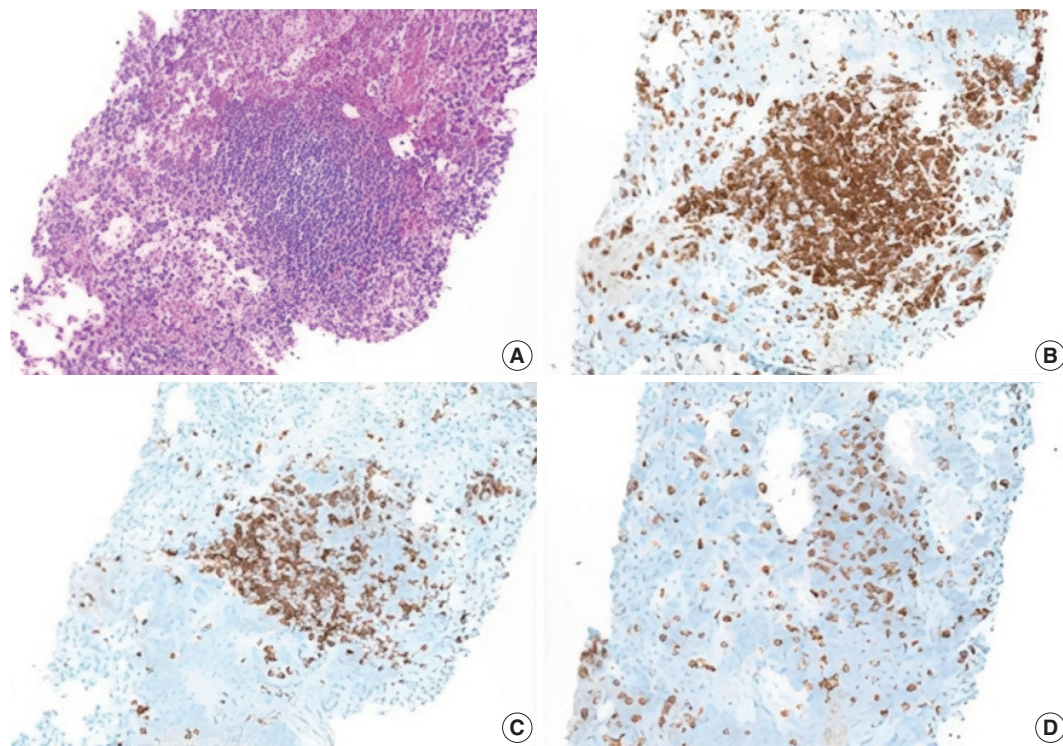


**Fig. 4.** Immunohistochemical staining of lymphoid aggregate. (A) Varying sized aggregates of small lymphoid cells were present in the lesion. (B) CD3 stains a moderate number of small T cells. (C) CD20 stains a small number of small B cells. (D) CD8 did not demonstrate organized lymphoid tissue.

acterized by anastomosing vascular spaces lined by bland, round-to-oval endothelial cells with scattered hobnail morphology. While cases have been reported in many organs, the kidney is most frequently affected [7]. AH is immunoreactive for CD34 and CD31 and negative for keratin [8]. AH shares many morphologic features as HSVN including the characteristic mutations in the G-protein subfamily [5]. However, AH is well-demarcated with no infiltrative growth.

Hepatic angiosarcoma (HAS) is the most common malignant mesenchymal liver tumor and is highly aggressive, with survival less than 6 months at time of diagnosis. Histologically, HAS displays infiltrating anastomosing vascular channels with tumor cells alongside dilated sinusoids. Endothelial cells may be round or spindle-shaped and exhibit severe nuclear atypia with frequent mitotic activity [9]. CD31 and CD34 are positive. Ki-67 levels are higher with a mean of 42.8% [3,4]. Thus, the Ki-67 proliferation index can be a useful distinction in differentiating these two neoplasms. Furthermore, the G-protein mutations seen in HSVN and AH are not found in HAS, which often has *TP53* or *KDR* mutations [6].

Different imaging modalities have been used in the workup of HSVN. Paisant et al. [2] reported possible characteristic imag-

ing findings in a case series involving four patients who underwent contrast-enhanced ultrasound (CEUS), computed tomography, and MRI. All modalities demonstrated similar enhancement patterns on arterial phase imaging with early, irregularly thick peripheral and continuous enhancement. The appearance at arterial phase on larger lesions was described as “flower petal shaped” due to early septa enhancement. Imaging-specific characteristics include persistent thick rim enhancement with mild central washout on CEUS and heterogenous hyperintensity on T2-weighted imaging [2]. However, there has been a case with innumerable enhancing lesions that were only visualized on the arterial phase [6].

While these radiological features are not totally diagnostic, they may be used to distinguish HSVN from other vascular hepatic lesions. For example, in classic hemangioma, there is peripheral, globular discontinuous enhancement as opposed to the thick rim, continuous enhancement seen in HSVN [2]. Hemangiomas also frequently display homogenous hyperintense T2 signal. AH shows nonspecific heterogenous, nodular enhancement [10]. HAS commonly shows heterogenous centripetal enhancement. It is also more likely to be poorly-circumscribed with a higher likelihood of intratumoral hemorrhage [11].

Unique to our case was the concern for hepatic splenosis or lymphoma. Splenosis is one type of ectopic spleen tissue, that typically occurs following abdominal trauma or splenectomy. Viable splenic tissue is autotransplanted in the abdominal cavity or more rarely in the thoracic cavity or brain. Hepatic splenosis is exceedingly rare and often asymptomatic with nonspecific imaging that can mimic other hepatic lesions [12]. CD8 stains a subset of T cells, and is useful for identifying splenic tissue because the endothelial cells lining the splenic sinuses are positive for CD8, a finding that is unique to those endothelial cells (littoral cells). In addition, there are case reports of contiguous primary marginal zone B-cell lymphoma and hemangioma [13]. The presumed T-cell predominant lymphoid aggregate in our HSVN case is not consistent with a marginal zone B-cell lymphoma and are more typical of reactive lymphoid aggregates.

Currently there are no treatment guidelines. While HSVN is considered a benign lesion, its full course is not understood, and the current recommendation is complete resection and close observation. The reported follow-up period is variable, with a mean of seven months. Both those with complete resection and those with positive margins showed no evidence of disease recurrence [14]. Long-term data is still needed to understand the disease course and guide definitive management.

### Ethics Statement

Institutional Review Board approval was waived due to the use of retrospective, de-identified data. This study adhered to the guidelines enacted by the Office of Human Research Protection that is supported by the U.S. Department of Health & Human Services. All information included in this report is de-identified and no personal details that may be used to identify the patient are included in this report. Written informed consent for the publication of this report was obtained from the patient.

### Availability of Data and Material

Data sharing not applicable to this article as no datasets were generated or analyzed during the study.

### Code Availability

Not applicable.

### ORCID

Madison Miranda <https://orcid.org/0009-0004-7843-3954>  
David Howell <https://orcid.org/0009-0005-7381-6216>  
Tony El Jabbour <https://orcid.org/0000-0002-6823-1919>

### Author Contributions

Conceptualization: TEJ. Investigation: MM. Supervision: TEJ. Writing—original draft: MM. Writing—review & editing: MM, DH, TEJ. Approval of final manuscript: all authors.

### Conflicts of Interest

The authors declare that they have no potential conflicts of interest.

### Funding Statement

No funding to declare.

### References

- Gill RM, Buelow B, Mather C, et al. Hepatic small vessel neoplasm, a rare infiltrative vascular neoplasm of uncertain malignant potential. *Hum Pathol* 2016; 54: 143-51.
- Paisant A, Bellal S, Lebigot J, Canivet CM, Michalak S, Aube C. Imaging features of hepatic small vessel neoplasm: case series. *Hepatology* 2021; 74: 2894-6.
- Walcott-Sapp S, Tang E, Kakar S, Shen J, Hansen P. Resection of the largest reported hepatic small vessel neoplasm. *Hum Pathol* 2018; 78: 159-62.
- Cicala CM, Monaca F, Giustiniani MC, Di Salvatore M. Multifocal hepatic small vessel neoplasm with spleen dissemination. *BMJ Case Rep* 2022; 15: e248785.
- Joseph NM, Brunt EM, Marginean C, et al. Frequent GNAQ and GNA14 mutations in hepatic small vessel neoplasm. *Am J Surg Pathol* 2018; 42: 1201-7.
- Akanuma N, Joseph NM, Stachler M, Behr S, Takahashi T, Gill RM. Malignant hepatic vascular neoplasm with novel RAF1 and GNA11 mutations: risk stratification considerations for hepatic small vessel neoplasm (HSVN). *Hum Pathol Rep* 2022; 29: 300671.
- Lappa E, Drakos E. Anastomosing hemangioma: short review of a benign mimicker of angiosarcoma. *Arch Pathol Lab Med* 2020; 144: 240-4.
- Lin J, Bigge J, Ulbright TM, Montgomery E. Anastomosing hemangioma of the liver and gastrointestinal tract: an unusual variant histologically mimicking angiosarcoma. *Am J Surg Pathol* 2013; 37: 1761-5.
- Bioulac-Sage P, Laumonier H, Laurent C, Blanc JF, Balabaud C. Benign and malignant vascular tumors of the liver in adults. *Semin Liver Dis* 2008; 28: 302-14.
- O'Neill AC, Craig JW, Silverman SG, Alencar RO. Anastomosing hemangiomas: locations of occurrence, imaging features, and diagnosis with percutaneous biopsy. *Abdom Radiol (NY)* 2016; 41: 1325-32.
- Liu Z, Yi L, Chen J, et al. Comparison of the clinical and MRI features of patients with hepatic hemangioma, epithelioid hemangioendothelioma, or angiosarcoma. *BMC Med Imaging* 2020; 20: 71.
- Kampa KC, Guerra JA, Percicotte AP, Zapparoli M, Raeder Costa MA, Ramos EJ. Hepatic splenosis: a report of a very rare case. *Gastroenterol Hepatol Open Access* 2019; 10: 88-91.
- Shiozawa K, Watanabe M, Ikehara T, et al. A case of contiguous primary hepatic marginal zone B-cell lymphoma and hemangioma ultimately diagnosed using contrast-enhanced ultrasonography. *Case Rep Oncol* 2015; 8: 50-6.
- Goh IY, Mulholland P, Sokolova A, Liu C, Siriwardhane M. Hepatic small vessel neoplasm: a systematic review. *Ann Med Surg (Lond)* 2021; 72: 103004.

# Diagnostic conundrums of schwannomas: two cases highlighting morphological extremes and diagnostic challenges in biopsy specimens of soft tissue tumors

Chankyung Kim<sup>1,2</sup>, Yang-Guk Chung<sup>3</sup>, Chan Kwon Jung<sup>4,5</sup>

<sup>1</sup>Department of Anatomical Pathology, SA Pathology, Adelaide, SA;

<sup>2</sup>Faculty of Health and Medical Sciences, University of Adelaide, Adelaide, SA, Australia;

Departments of <sup>3</sup>Orthopedic Surgery and <sup>4</sup>Hospital Pathology, College of Medicine, The Catholic University of Korea, Seoul;

<sup>5</sup>Cancer Research Institute, College of Medicine, The Catholic University of Korea, Seoul, Korea

Schwannomas are benign, slow-growing peripheral nerve sheath tumors commonly occurring in the head, neck, and flexor regions of the extremities. Although most schwannomas are easily diagnosable, their variable morphology can occasionally create difficulty in diagnosis. Reporting pathologists should be aware that schwannomas can exhibit a broad spectrum of morphological patterns. Clinical and radiological examinations can show correlation and should be performed, in conjunction with ancillary tests, when appropriate. Furthermore, deferring a definitive diagnosis until excision may be necessary for small biopsy specimens and frozen sections. This report underscores these challenges through examination of two unique schwannoma cases, one predominantly cellular and the other myxoid, both of which posed significant challenges in histological interpretation.

**Key Words:** Neurilemmoma; Soft tissue neoplasms; Biopsy; Frozen sections; Immunohistochemistry; Pathologists; Extremities; Mitosis

**Received:** June 17, 2023 **Revised:** July 9, 2023 **Accepted:** July 13, 2023

**Corresponding Author:** Chan Kwon Jung, MD, PhD, Department of Pathology, Seoul St. Mary's Hospital, College of Medicine, The Catholic University of Korea, 222 Banpo-daero, Seocho-gu, Seoul 06591, Korea

Tel: +82-2-2258-1622, Fax: +82-2-2258-1627, E-mail: ckjung@catholic.ac.kr

Schwannomas are slow-growing, benign peripheral nerve sheath tumors that occur commonly in the head and neck region or flexor aspects of the extremities. Schwannomas also can occur, but are not limited to, the spinal or paraspinal region, cranial nerves, central nervous system, viscera, and bone. While more than 90% of cases are solitary and sporadic, multiple paraspinal schwannomas or involvement of the eight cranial nerves suggests neurofibromatosis 2 (NF2), and bilateral vestibular schwannoma is diagnostic of NF2. It is well known that tumorigenesis of schwannomas is due to the loss of merlin, a product of the *NF2* gene, located at 22q2.2 [1].

A broad range of histological patterns can be observed in schwannomas, and the 5th edition of the World Health Organization Classification of soft tissue and bone tumors recognizes ancient, cellular, plexiform, epithelioid, and microcystic/reticular subtypes. Conventional schwannomas are composed almost entirely or entirely of Schwann cells with spindle morphology

and typically exhibit Antoni A, Antoni B, and Verocay bodies. Although schwannomas are easily diagnosable on most occasions without ancillary testing, obtaining the correct diagnosis can be difficult due to their variable morphology.

Herein, we report two cases of schwannomas that exhibited histological features that were at opposite ends of the morphological spectrum, with differing cellularity and nuclear atypia, resulting in challenging biopsy and intraoperative frozen section interpretations.

## CASE REPORT

### Case 1

A 68-year-old male with no known medical or surgical history was referred to a tertiary hospital due to a left thigh mass that the patient had first noticed 3 years prior and that had recently increased in size. Additionally, two other masses were observed

adjacent to the primary mass. The physical examination revealed no neurovascular compromise.

Magnetic resonance imaging (MRI) revealed a heterogeneously enhancing mass situated at the anterior aspect of the left thigh within the subcutaneous tissue plane. The largest of the masses exhibited central cystic changes and measured 7 cm at its maximum dimension, raising the possibility of a malignant soft tissue tumor (Fig. 1A).

A core needle biopsy was performed to rule out a malignant soft tissue neoplasm. The biopsy revealed densely packed short to long sweeping fascicles of spindle cells exhibiting marked hypercellularity and acellular degenerated areas (Fig. 1B). The tu-

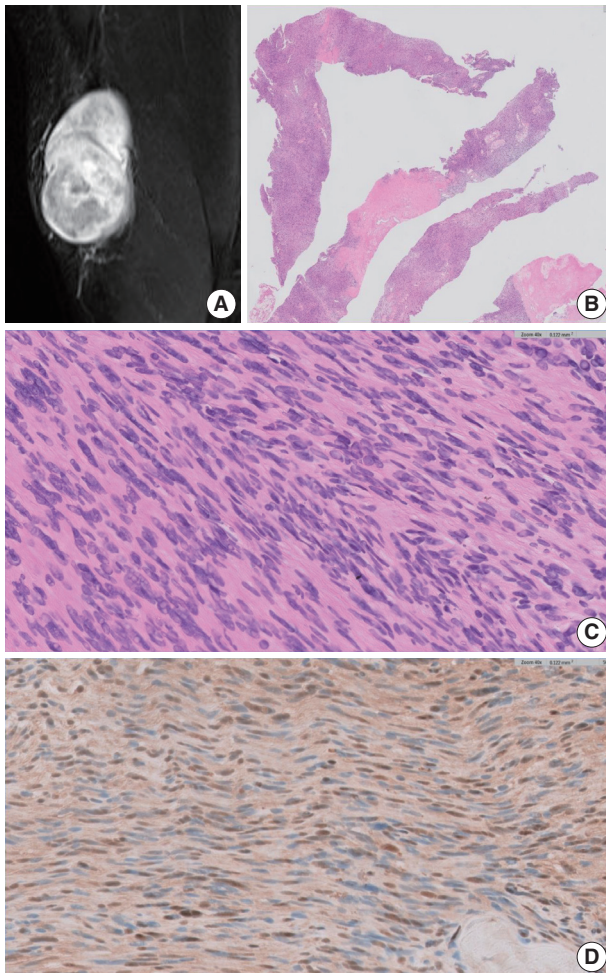


**Fig. 1.** A cellular schwannoma. (A) Magnetic resonance imaging scan showing a heterogeneously enhancing mass within the subcutaneous tissue plane. (B) Core biopsies showing predominantly cellular areas, resulting in a “blue appearance” accompanied by pale degenerate areas. (C) Compact spindle cells showing hypercellularity and mild nuclear pleomorphism. (D) S-100 immunohistochemistry showing a focal weak staining pattern despite high cellularity.

mor cells exhibited mild nuclear pleomorphism (Fig. 1C). S-100 immunohistochemistry (IHC) revealed positive staining in the tumor cells, with some areas exhibiting a weak staining pattern (Fig. 1D). The tumor cells also demonstrated diffuse strong positivity for SOX10, CD56, and CD99 while being negative for actin, desmin, pan-cytokeratin, epithelial membrane antigen, and CD34. Consequently, the biopsy results were not entirely conclusive, and a malignant peripheral nerve sheath tumor (MPNST) could not be definitively ruled out.

Upon gross examination of the excised specimen, the largest tumor was well surrounded by a thin fibrous capsule. The cut surface exhibited a solid yellow-to-tan appearance with cystic changes (Fig. 2A). The microscopic findings showed heterogeneous morphological patterns, including hypercellular regions lacking Verocay bodies (Fig. 2B) and areas characteristic of classic schwannoma. Rare mitotic figures were detected at 1 per mm<sup>2</sup> (Fig. 2C) with a Ki-67 labeling index less than 5% (Fig. 2D). The final diagnosis of cellular schwannoma was made based on excision.

## Case 2

A 72-year-old female with a medical history of rheumatoid arthritis and no prior surgical interventions was referred to a tertiary care hospital due to a slow-growing mass in her left forearm that had been present for 4 years. The physical examination yielded an equivocal result on the Tinel test. MRI revealed a T2-bright mass demonstrating heterogeneous enhancement. The mass, measuring 12.3 cm at its maximum dimension, was suggestive of a benign peripheral nerve sheath tumor (Fig. 3A).

During surgery, a frozen section examination of three areas of the tumor exhibited an entirely myxoid, paucicellular pattern (Fig. 3B, C). The interim interpretation identified it as a low-grade myxoid tumor with a final determination deferred until the permanent sections could be evaluated.

Upon gross examination of the excised specimen, the tumor was well-circumscribed, exhibiting a myxoid peripheral zone and a more solid, yellowish central area (Fig. 4A). Histopathological examination revealed a paucicellular area on the tumor’s superficial aspect, characterized by loose myxoid stroma interspersed with scattered spindle cells exhibiting wavy nuclei (Fig. 4B, C). These cells exhibited positive labeling with S-100 IHC. Deeper within the tumor, a region more characteristic of a conventional schwannoma was identified (Fig. 4B). The final diagnosis was schwannoma with myxoid change.



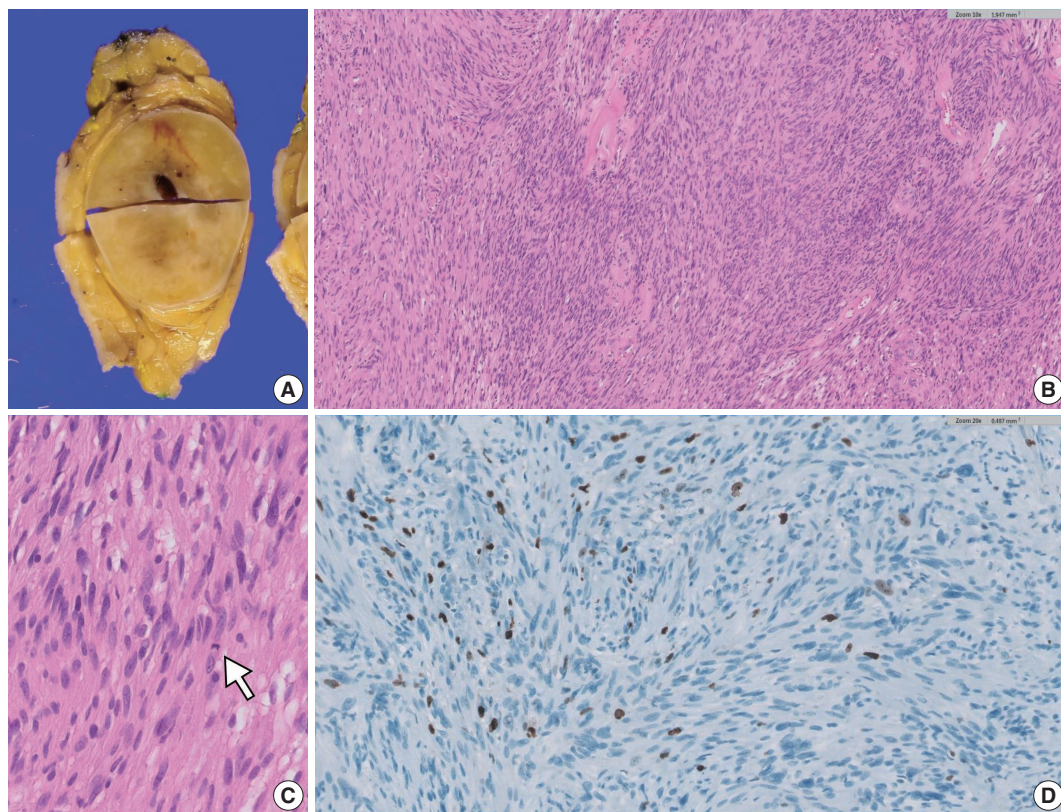


**Fig. 2.** Excision specimen of a cellular schwannoma. (A) Solid yellow-to-tan lesion with a surrounding thin fibrous capsule. (B) Hypercellular region without well-formed Verocay bodies. (C) One of the rare mitotic figures detected (white arrow). (D) Ki-67 labelling index less than 5%.

## DISCUSSION

Cellular schwannomas, as the name suggests, exhibit higher cellularity and increased mitotic figures compared to conventional schwannomas, although the mitotic count is typically less than 5 mitoses/mm<sup>2</sup>. These also typically reveal the absence of Verocay bodies and may exhibit hyperchromasia and microscopic foci of necrosis, further complicating the histological interpretation [2] and raising the possibility of malignant spindle cell neoplasms such as MPNST. Well-formed capsule and subcapsular lymphoid aggregates may support the diagnosis of schwannoma, but they are not always present. For this reason, additional ancillary tests are often required in this setting, and less diffuse reactivity with S-100 and loss of H3K27me<sub>3</sub> by IHC are evidence against the diagnosis of schwannoma and favor MPNST [3].

In case 1, where a pre-operative diagnosis was obtained from a small biopsy, a retrospective analysis revealed characteristics suggestive of cellular schwannoma. However, this diagnosis was challenging due to the absence of hypocellular areas and Verocay bodies, and S-100 IHC did not demonstrate diffuse strong positivity. Although the mitotic count could have been informative

in excluding MPNSTs [2], it remains an unreliable measure in biopsy specimens. Low-grade MPNSTs typically exhibit cytological atypia, hypercellularity, a mitotic count ranging from 1.5 to 4.5 mitoses/mm<sup>2</sup> (equivalent to 3–9 mitotic figures per 10 high-power fields), and the absence of necrosis [4]. However, in the present case, the surgical specimen demonstrated only 1 mitosis per mm<sup>2</sup>, which falls below the diagnostic criteria for low-grade MPNST. Mitotic activity can be observed in cellular schwannomas but is typically less than 5 per 10 high-power fields [5]. Brisk mitotic activity may be present in rare instances, potentially exceeding 10 per 10 high-power fields [5]. However, if other diagnostic features of cellular schwannoma are present, this heightened proliferative activity remains aligned with a benign diagnosis. Cellular schwannomas are characterized by a specific pattern of Ki-67 labeling, primarily manifesting in the form of localized hotspots rather than a diffused increment [2]. Even in the presence of these hotspots, the Ki-67 index seldom exceeds 20%. The utilization of a Ki-67 stain can reveal variable labeling indices throughout a cellular schwannoma, with a significant concentration in hotspot regions [2]. By contrast, the Ki-67 stain typically exhibits a diffusely elevated labeling pattern in the con-

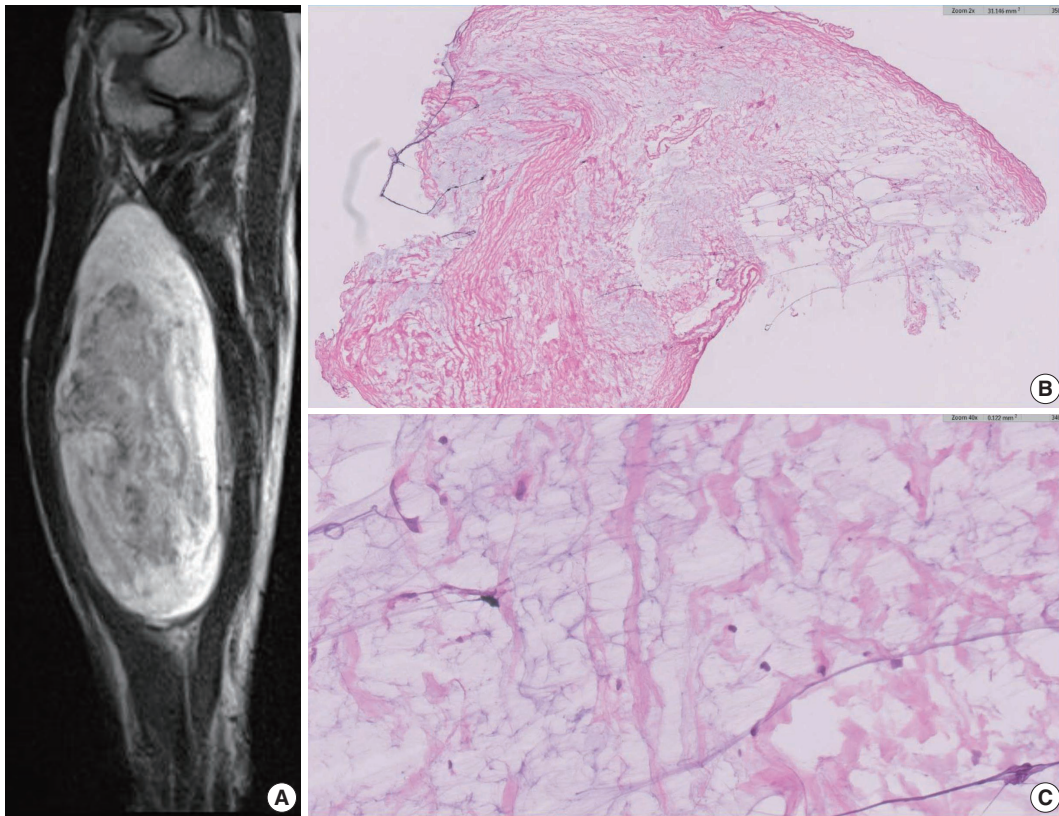


**Fig. 3.** A schwannoma with myxoid change. (A) Magnetic resonance imaging showing a T2-bright mass displaying heterogeneous enhancement. (B, C) Low- and high-power views of the frozen section showing scattered cytologically benign spindle cells with surrounding loose myxoid stroma.

text of an MPNST.

Although the identification of H3K27me3 loss can assist in confirming a diagnosis of high-grade MPNST, the presence of positive staining does not preclude the possibility of MPNST, as only 34% of cases demonstrated a loss of staining in a study conducted by Cleven et al. [3]. Moreover, H3K27me3 antibodies are not readily accessible in many settings. Consequently, it is often challenging to conclusively diagnose cellular schwannoma based solely on a small biopsy sample.

S-100 is a common, widely-used antibody for diagnostic use in histopathology as a neural marker, and it is useful in differentiating schwannomas and MPNSTs, as schwannomas typically exhibit diffuse and strong positivity, while MPNSTs demonstrate patchy or negative staining [5]. However, such a description is arbitrary, and there are no defined criteria on how diffuse and strong the staining has to be in a numerical or percentage form. There was focal weak staining with S-100 IHC in our cellular schwannoma case, which was problematic. Pekmezci et al. [2] used 90% as a cutoff value for diffuse positive staining and <5% for negative staining for a comparison between schwannomas and

MPNSTs. No intensity of staining was documented. In Pekmezci et al. [2], 96% of cellular schwannomas stained diffusely, while only 14% of MPNSTs revealed diffuse positivity. With such findings, the authors believe the 90% cutoff value to be useful when used in conjunction with morphological and radiological evaluations.

Myxoid change is a well-described phenomenon in schwannomas and often causes diagnostic difficulties [6]. Case 2 revealed extensive myxoid change, particularly within the peripheral aspect of the tumor, and led to a diagnostic dilemma during the intraoperative frozen section. Chaurasia et al. [6] described a reticular schwannoma mimicking a low-grade fibromyxoid sarcoma, and this case also described extensive myxoid change. Many soft tissue tumors can exhibit myxoid change. For this reason, in small biopsy specimens of such cases, it would be prudent to report such cases as a low-grade myxoid neoplasm and recommend complete excision for a definitive assessment unless there are unequivocal histological features of schwannomas, including Antoni A, Antoni B, and Verocay bodies.

Interestingly, even after multiple incisional biopsies were per-

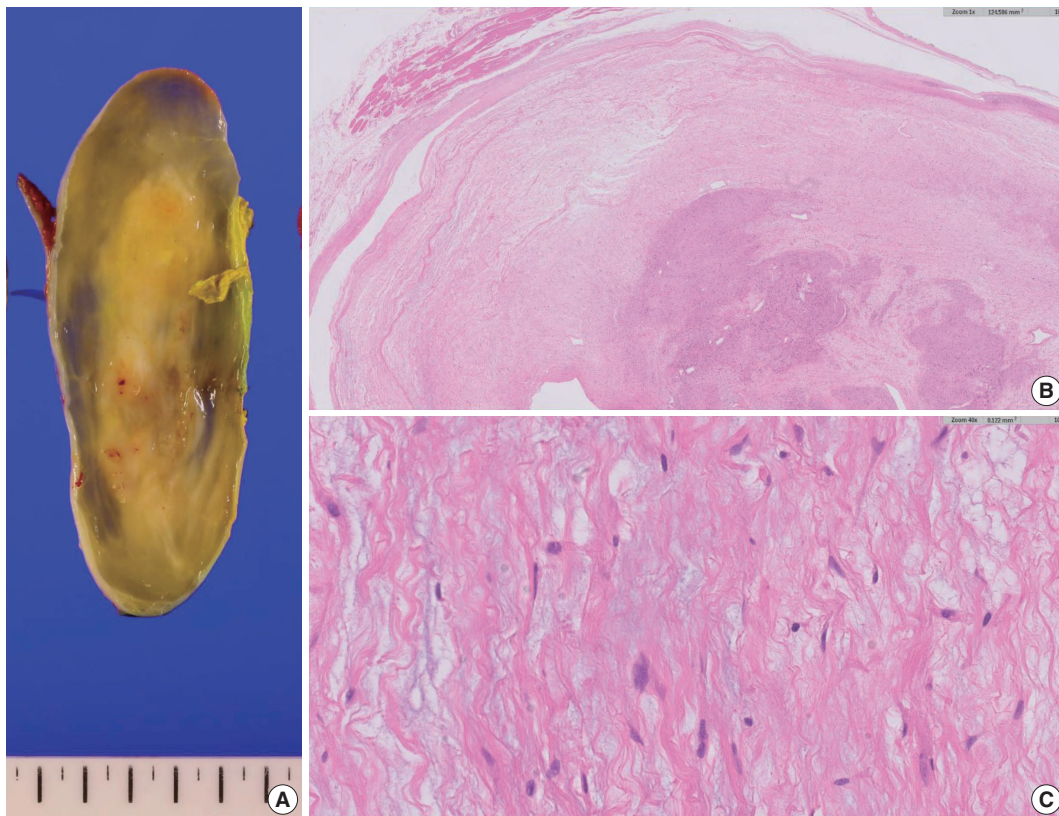


**Fig. 4.** Excision specimen of a schwannoma with myxoid change. (A) Well-circumscribed, demonstrating a solid central area with a myxoid peripheral zone. (B) Interface between the loose myxoid area and more classic schwannoma-like area. Note that the classic area is observed at the deeper aspect. (C) High-power view exhibiting scattered spindle cells within the myxoid stroma.

formed for intraoperative frozen section of case 2, no diagnostic material for a schwannoma was obtained. The European Society for Medical Oncology (ESMO) guidelines [7] suggest that multiple core needles using 14 or greater gauge needles are used to sample different tumor locations and depths, correlating with radiological imaging. In hindsight, if the biopsies were performed from both superficial and deep aspects for this case, instead of multiple superficial biopsies only; these may have captured a more diagnostic area of the schwannoma.

Identifying extremely T2-bright and T1-hypointense enhancing lesions on MRIs involving the extremities or, less commonly, the trunk without visceral involvement suggests a myxoid neoplasm. However, these findings can also be observed in schwannomas [8]. The other radiological signs that can be seen in schwannomas include a fat split sign and a target sign [9]. For these reasons, correlation with radiological findings may be helpful in distinguishing between other myxoid neoplasms from a schwannoma with myxoid change.

A study by Pianta et al. [10] described 100% concordance between biopsy and excision in 41 cases of peripheral nerve sheath

tumors, substantiating the accuracy of a core biopsy. Furthermore, a meta-analysis by Birgin et al. [11] revealed 88% sensitivity and 77% specificity for soft tissue sarcoma histotypes, further verifying the usefulness and high accuracy of core needle biopsies. However, histological heterogeneity is well known in soft tissue tumors [12], and obtaining a non-representative sample remains possible. Therefore, a definitive diagnosis is often deferred until after excision.

Reporting pathologists should be aware that a broad spectrum of morphological patterns in schwannomas can lead to a diagnostic challenge. Clinical and radiological exams and judicious use of ancillary tests is recommended when appropriate. Furthermore, deferring a definitive diagnosis to excision may be necessary for small biopsy specimens and frozen sections.

#### Ethics Statement

Formal written informed consent was not required with a waiver by the appropriate IRB (KC23ZASI0457).

#### Availability of Data and Material

Data sharing is not applicable to this article as no datasets were generated

or analyzed during the study.

### Code Availability

Not applicable.

### ORCID

Chankyung Kim <https://orcid.org/0000-0001-6054-0605>  
 Yang-Guk Chung <https://orcid.org/0000-0001-8153-8205>  
 Chan Kwon Jung <https://orcid.org/0000-0001-6843-3708>

### Author Contributions

Conceptualization: CKJ. Data curation: CK, YGC, CKJ. Formal analysis: CK, CKJ. Investigation: CK, YGC, CKJ. Supervision: CKJ. Writing—original draft: CK, CKJ. Writing—review & editing: CK, YGC, CKJ. Approval of final manuscript: all authors.

### Conflicts of Interest

C.K.J., the editor-in-chief of the *Journal of Pathology and Translational Medicine*, was not involved in the editorial evaluation or decision to publish this article. All remaining authors have declared no conflicts of interest.

### Funding Statement

This research was supported by a grant (HI21C0940) from the Korean Health Technology R&D Project, Ministry of Health and Welfare, Republic of Korea.

### References

1. WHO Classification of Tumours Editorial Board. WHO classification of tumours: soft tissue and bone tumours. 5th ed. Lyon: International Agency for Research on Cancer, 2020.
2. Pekmezci M, Reuss DE, Hirbe AC, et al. Morphologic and immunohistochemical features of malignant peripheral nerve sheath tumors and cellular schwannomas. *Mod Pathol* 2015; 28: 187-200.
3. Cleven AH, Sannaa GA, Briaire-de Bruijn I, et al. Loss of H3K27 tri-methylation is a diagnostic marker for malignant peripheral nerve sheath tumors and an indicator for an inferior survival. *Mod Pathol* 2016; 29: 582-90.
4. Miettinen MM, Antonescu CR, Fletcher CD, et al. Histopathologic evaluation of atypical neurofibromatous tumors and their transformation into malignant peripheral nerve sheath tumor in patients with neurofibromatosis 1: a consensus overview. *Hum Pathol* 2017; 67: 1-10.
5. Rodriguez FJ, Folpe AL, Giannini C, Perry A. Pathology of peripheral nerve sheath tumors: diagnostic overview and update on selected diagnostic problems. *Acta Neuropathol* 2012; 123: 295-319.
6. Chaurasia JK, Afroz N, Sahoo B, Naim M. Reticular schwannoma mimicking myxoid sarcoma. *BMJ Case Rep* 2014; 2014: bcr2013202963.
7. Casali PG, Abecassis N, Aro HT, et al. Soft tissue and visceral sarcomas: ESMO-EURACAN Clinical Practice Guidelines for diagnosis, treatment and follow-up. *Ann Oncol* 2018; 29: iv51-67.
8. Baheti AD, Tirumani SH, Rosenthal MH, et al. Myxoid soft-tissue neoplasms: comprehensive update of the taxonomy and MRI features. *AJR Am J Roentgenol* 2015; 204: 374-85.
9. Lee E, Lee GY, Cho WS, et al. Useful MRI features for distinguishing benign peripheral nerve sheath tumors and myxoid tumors in the musculoskeletal system. *Investig Magn Reson Imaging* 2015; 19: 153-61.
10. Pianta M, Chock E, Schlicht S, McCombe D. Accuracy and complications of CT-guided core needle biopsy of peripheral nerve sheath tumours. *Skeletal Radiol* 2015; 44: 1341-9.
11. Birgin E, Yang C, Hetjens S, Reissfelder C, Hohenberger P, Rahbari NN. Core needle biopsy versus incisional biopsy for differentiation of soft-tissue sarcomas: a systematic review and meta-analysis. *Cancer* 2020; 126: 1917-28.
12. Mitsuyoshi G, Naito N, Kawai A, et al. Accurate diagnosis of musculoskeletal lesions by core needle biopsy. *J Surg Oncol* 2006; 94: 21-7.

## *EWSR1* rearranged primary renal myoepithelial carcinoma: a diagnostic conundrum

Nilay Nishith, Zachariah Chowdhury

Department of Onco-Pathology, Mahamana Pandit Madan Mohan Malviya Cancer Centre, Varanasi, India

Primary renal myoepithelial carcinoma is an exceedingly rare neoplasm with an aggressive phenotype and Ewing sarcoma breakpoint region 1 (*EWSR1*) rearrangement in a small fraction of cases. In addition to its rarity, the diagnosis can be challenging for the pathologist due to morphologic heterogeneity, particularly on the biopsy specimen. At times, immunohistochemistry may be indecisive; therefore, molecular studies should be undertaken for clinching the diagnosis. We aim to illustrate a case of primary myoepithelial carcinoma of the kidney with *EWSR1*-rearrangement in a 67-year-old male patient who presented with right supraclavicular mass, which was clinically diagnosed as carcinoma of an unknown primary. An elaborate immunohistochemical work-up aided by fluorescent in-situ hybridization allowed us to reach a conclusive diagnosis. This unusual case report advocates that one should be aware of the histological mimickers and begin with broad differential diagnoses alongside sporadic ones and then narrow them down with appropriate ancillary studies.

**Key Words:** *EWSR1* gene rearrangement; Kidney; Myoepithelial carcinoma; Prognosis

**Received:** May 24, 2023 **Revised:** July 9, 2023 **Accepted:** August 8, 2023

**Corresponding Author:** Nilay Nishith, MD, DNB (Pathology), Department of Onco-Pathology, Mahamana Pandit Madan Mohan Malviya Cancer Centre, BHU Campus, Sundarapur, Varanasi, Uttar Pradesh - 221005, India  
 Tel: +91-9900241232, E-mail: [drmilynishith@gmail.com](mailto:drmilynishith@gmail.com)

Myoepitheliomas are soft tissue neoplasms composed either exclusively or predominantly of cells exhibiting myoepithelial phenotype. They are known to arise in a wide range of locations such as the skin, salivary gland, lung, and gastrointestinal tract. The malignant counterpart of these neoplasms (i.e. myoepithelial carcinoma) also shows a similar anatomic distribution and displays a plethora of histomorphological patterns [1,2]. Primary renal myoepithelial carcinomas are exceedingly rare, with only four cases described in the English literature [2–4]. In addition to its rarity, the diagnosis can be challenging for the pathologist due to morphologic heterogeneity, particularly on the biopsy specimen. The present case report aims to showcase primary myoepithelial carcinoma (MEC) of the kidney with Ewing sarcoma breakpoint region 1 (*EWSR1*)-rearrangement in a 67-year-old male patient who presented with right supraclavicular mass, which was clinically diagnosed as carcinoma of an unknown primary (CUP). This case report also incorporates a detailed account of the clinical, pathological, immunohistochemical, and molecular aspects, with an emphasis on the challenges encountered

while diagnosing such a rare neoplasm.

### CASE REPORT

A 67-year-old male patient presented to the head and neck outpatient department with a right supraclavicular mass. His baseline hematological investigation revealed severe anemia and neutrophilic leukocytosis. Subsequently, the right supraclavicular mass was sampled and sent for histopathological assessment. Microscopic examination favored a benign neoplasm, with the cells arranged in cords, trabeculae, tubules and singly scattered over a loose myxoid stroma. These cells were oval to spindle-shaped and possessed largely monomorphic nuclei, dispersed chromatin, inconspicuous nucleoli, and a scant to moderate amount of eosinophilic cytoplasm (Fig. 1A, B). Nuclear atypia, necrosis, or increased mitotic activity were absent. On immunohistochemistry, the neoplastic cells were positive for AE1/AE3, smooth muscle actin (SMA), and p63 (Fig. 1C, D) while were negative for cytokeratin (CK) 7, CK20, S-100, calponin, paired box 8 (PAX8),

NKX3.1, NKX2.2, and TLE-1. Integrase interactor 1 (INI-1) expression was retained in these cells. Thus, a diagnosis of myoepithelioma was rendered. Further, positron emission tomography and computed tomography (PET-CT) was performed, which showed a fluorodeoxyglucose (FDG) avid right supraclavicular mass (eroding the medial end of the clavicle and impinging on the right thyroid lobe); measuring 75 × 61 mm, SUVmax 5.55 (Fig. 2A, B) along with FDG avid mass noted involving the upper pole and interpolar region of the left kidney; measuring 62 × 52 mm, SUVmax 10.26 (Fig. 2C, D). Hypermetabolic metastatic retroperitoneal lymph nodes, left adrenal, and lytic skeletal lesions were also present. The renal mass was also sampled to discriminate between a metastasis to the kidney versus a second primary. Microscopically, the cores of renal parenchyma exhibited infiltration by a tumor disposed in nests and sheets. The neoplastic cells are round, with a high nucleo-cytoplasmic ratio, fine to vesicular nuclei, prominent nucleoli, and scant cytoplasm (Fig. 3A, B). Brisk mitotic activity, tumor cell apoptosis, and areas of necrosis were also noted. Immunostaining showed positivity for AE1/AE3, SMA, CD10, p63 (Fig. 3C–F), while they were negative for PAX8, TFE3, S100, ALK1, HMB45, carbonic anhydrase IX, and vimentin. INI1 expression was retained in the tumor cells. Considering the findings of PET-CT, the report was

validated as primary renal myoepithelial carcinoma with metastatic right supraclavicular mass. Subsequently, the left renal mass biopsy was subjected to fluorescent in-situ hybridization (FISH), which showed *EWSR1* rearrangement (Fig. 4). He is being managed by the Department of Medical Oncology and has been offered the option of supportive care as the best alternative in view of the extensive disease burden, skeletal metastasis, and nodal involvement.

## DISCUSSION

Primary renal myoepithelial carcinoma is a rare tumor, which was first described in 1998, and since then, there have been only a few reported cases in the literature. It typically presents with nonspecific symptoms such as abdominal pain, hematuria, and flank mass [2–4]. Imaging studies, such as computed tomography or magnetic resonance imaging, are often used to diagnose and stage the tumor. However, these imaging modalities are not specific for malignant myoepithelioma and may lead to a misdiagnosis at both usual and uncommon sites such as the kidney [2,3,5,6].

Renal myoepithelial carcinomas have overlapping histological features and share similarities with their soft tissue counterpart.

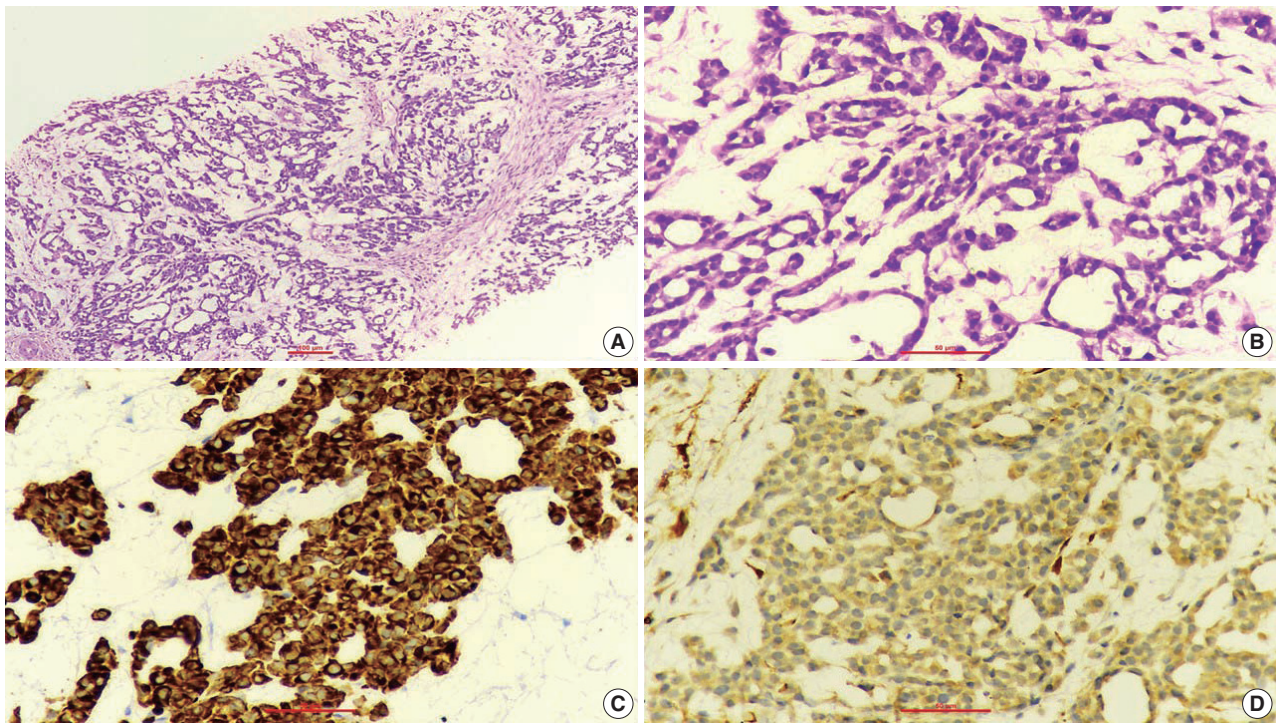


**Fig. 1.** The neoplastic cells are arranged in cords, trabeculae, tubules and scattered singly over a loose myxoid stroma (A). The neoplastic cells are oval to spindle-shaped and possess largely monomorphic nuclei, dispersed chromatin, inconspicuous nucleoli, and a scant to moderate amount of eosinophilic cytoplasm (B). The neoplastic cells are positive for AE1/AE3 (C) and smooth muscle actin (D).

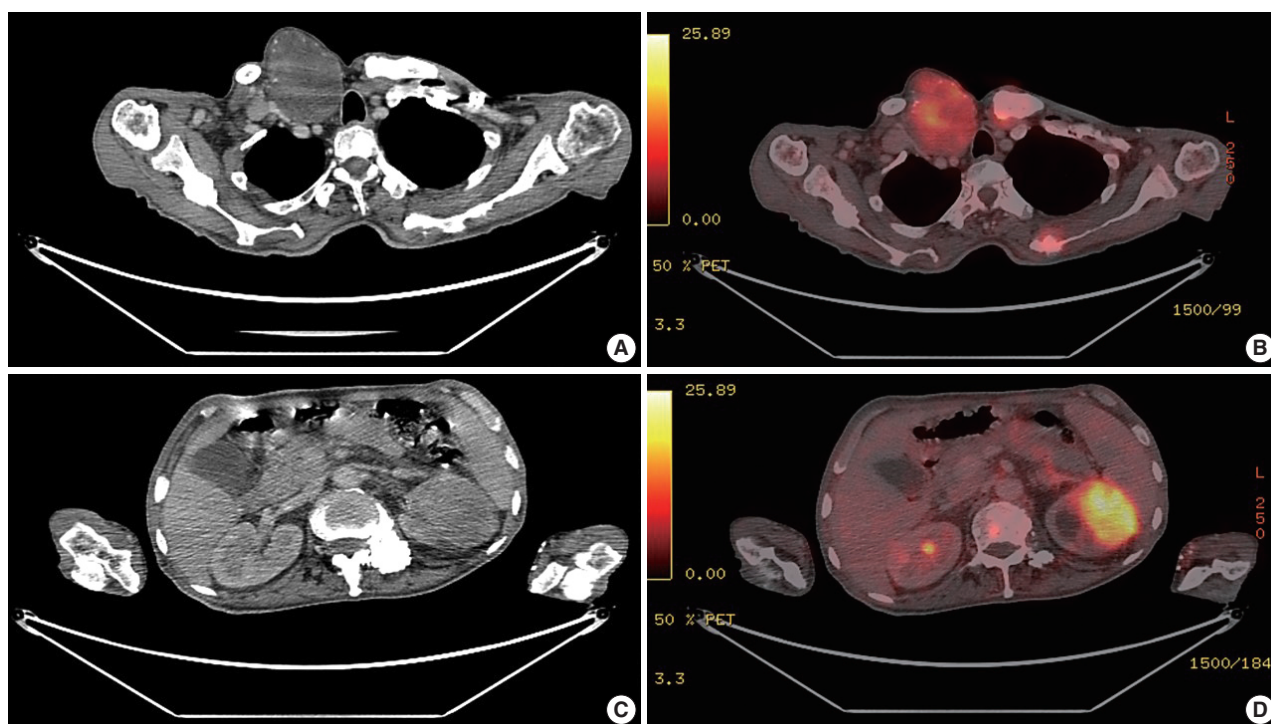


**Fig. 2.** Positron emission tomography and computed tomography (PET-CT) images of the hypermetabolic right supraclavicular mass (A, B). PET-CT images of the left renal lesion (C, D).

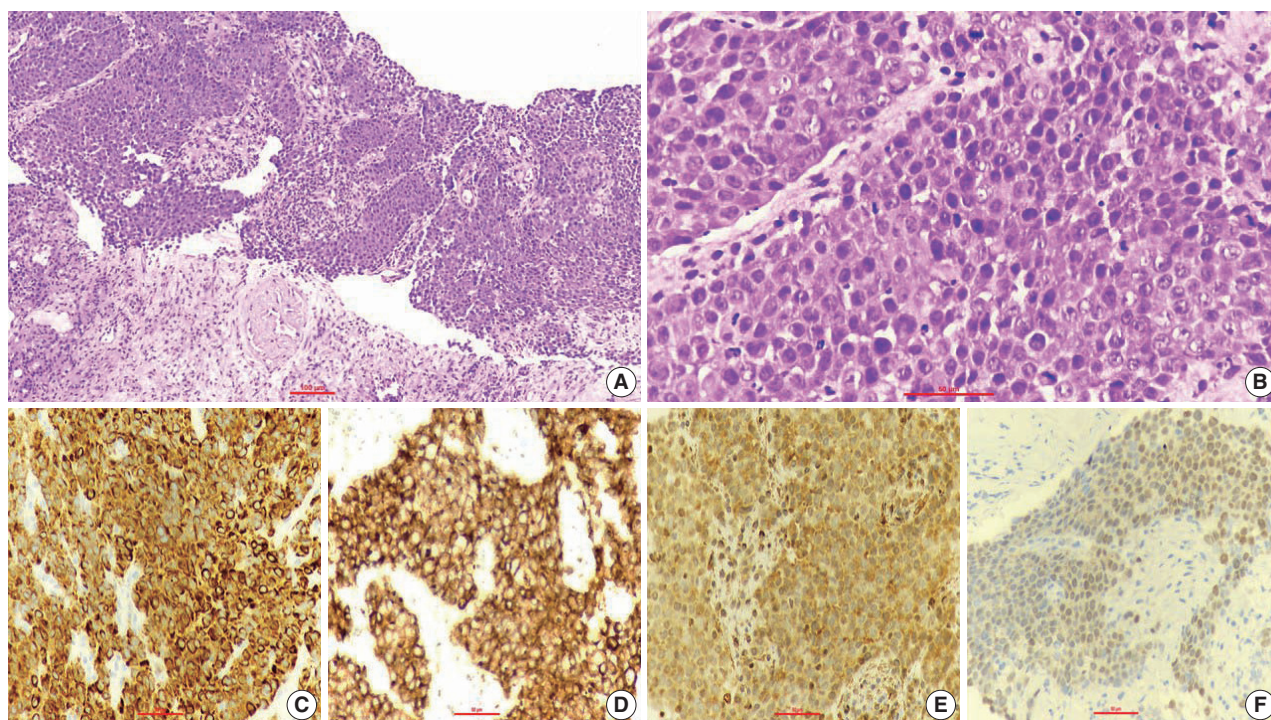


**Fig. 3.** The tumor cells are disposed in nests and sheets (A). The tumor cells are round, with a high nucleo-cytoplasmic ratio, fine to vesicular nuclei, prominent nucleoli, and scant cytoplasm (B). The tumor cells are positive for AE1/AE3 (C), CD10 (D), smooth muscle actin (E), and p63 (F).

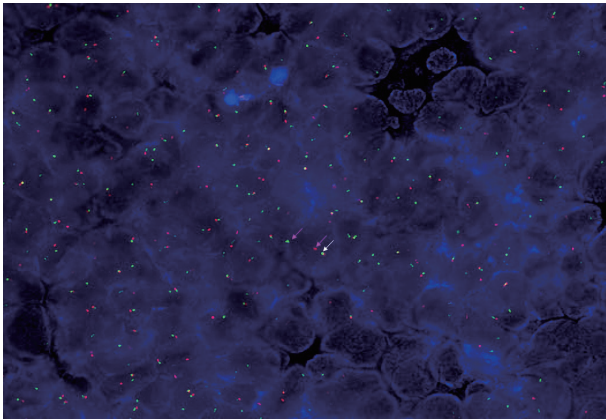


**Fig. 4.** Fluorescent in-situ hybridization using dual-color break-apart probe illustrating Ewing sarcoma breakpoint region 1 (*EWSR1*) gene rearrangement. The pink arrows indicate separated (split) red and green signals denoting a rearrangement involving the *EWSR1* gene at 22q12. The white arrow points toward a normal fused signal, which is the site of the *EWSR1* gene.

These are characterized by variable combinations of distinct cellular and stromal components. Different cell types (epithelioid, spindled, plasmacytoid, and clear) can be appreciated in variable proportions and are arranged in cords, trabeculae, solid sheets, and occasionally ducts. The cellular component is embedded in a myxoid/chondromyxoid to hyalinized stroma, with occasional frank chondroid and osseous differentiation. Immunohistochemical studies reveal that the neoplastic cells express myoepithelial markers in variable degrees, including smooth muscle actin, calponin, CD10, and p63. Thus, a diagnosis of malignant myoepithelioma is rendered based on histological and immunohistochemistry findings [1,5,7]. In addition, molecular analysis may help establish the diagnosis, as some cases have been found to harbor *EWSR1* rearrangements. Recent studies have identified *EWSR1* rearrangements as a potential pathologic mechanism underlying this unusual neoplasm. *EWSR1* rearrangement involves the fusion of the *EWSR1* gene with a partner gene, such as *PBX1*, *ZNF444*, *KLF15*, or *POU5F1* [8-12]. This fusion event results in the formation of an *EWSR1* fusion protein, which plays a crucial role in the pathogenesis of primary renal myoepithelial carcinoma. The *EWSR1* fusion protein interacts with transcription factors, such as CREB1 and ATF1, and regulates downstream target genes involved in cell proliferation and survival. *KLF15* plays a crucial role in podocyte differentiation, mesangial cell proliferation, and renal fibrosis modulation in the kidney. Distal tubular, collecting duct, mesangial epithelial cells, and renal cortical fibroblasts also express *KLF15*. Based on these observations, it may be speculated that the manifestation of an *EWSR1::KLF15*

fusion within the kidney as MEC could be organ-specific. However, the clinical significance of *EWSR1* rearrangements in malignant myoepithelioma remains unclear [2,3,11,12].

The rarity of primary renal myoepithelial carcinoma poses a diagnostic challenge for clinicians as well as pathologists. The tumor may be misdiagnosed as other renal malignancies, such as renal cell carcinoma, collecting duct carcinoma, and sarcomatoid renal cell carcinoma. Immunohistochemistry studies are essential to differentiate myoepithelial carcinoma from these histological mimickers. Further, molecular studies, particularly *EWSR1* rearrangement analysis, may help in clinching the diagnosis. The identification of these exceptionally rare neoplasms becomes furthermore challenging on biopsy samples. Therefore, it is a good practice to start with broad differential diagnoses alongside sporadic ones and then narrow them down with the assistance of immunohistochemistry.

In the present case, the initial work-up revealed myoepithelioma of soft tissue origin in the right supraclavicular region. Subsequently, he was thoroughly investigated and found to have a large renal mass with SUVmax greater than the soft tissue lesion, indicating that the former is more metabolically active than the latter and hence, has a higher propensity to metastasize. The histopathological analysis of the renal mass is revealed to be myoepithelial carcinoma exhibiting brisk mitotic activity, tumor cell apoptosis, and areas of necrosis. An extensive panel of immunohistochemical markers was used to exclude all possible differential diagnoses, including primary renal neoplasms and metastatic lesions. Finally, in conjunction with PET-CT findings, he was diagnosed with primary renal myoepithelial carcinoma with metastatic right supraclavicular mass. The diagnosis was confirmed on FISH using *EWSR1* break-apart probe. Another pertinent point to note is that the histomorphological characteristics of the primary and metastatic lesions are not the same. This difference could be attributed to the fact that both lesions were large and were diagnosed on biopsy specimens. Therefore, it may be possible that both masses display different histological features owing to the morphological heterogeneity of myoepithelial carcinoma, site of biopsy, and differences in metabolic activity as indicated by SUVmax. An extensive literature search revealed that three of the four prior cases also presented with distant metastasis (mainly lung) at the time of diagnosis [2-4]. However, none have commented upon the histology of the metastatic lesions. On the other hand, we have detailed the histological features of both primary and metastatic lesions and emphasized the differences and the likely reasons for the same.

The existing literature about primary renal myoepithelial car-



cinoma is very limited and is available in the form of mere case reports. A thorough appraisal of the published articles indicates that these are highly aggressive tumors with poor prognosis. Surgery remains the mainstay of treatment, and radical nephrectomy is recommended for localized disease. Adjuvant chemotherapy and/or radiotherapy may be considered for high-risk cases or metastatic disease, although their efficacy is uncertain. There is currently no standard systemic therapy for primary renal myoepithelial carcinoma, and clinical trials are urgently needed to develop effective treatment strategies [2-4].

Primary renal myoepithelial carcinoma is a rare and aggressive tumor, and a subset of these neoplasms show *EWSR1* gene rearrangement. The biphasic histology and characteristic immunophenotype help to distinguish MEC from other renal neoplasms. Molecular studies are crucial for accurately diagnosing this malignancy and differentiating it from its histological mimickers. Surgery remains the mainstay of treatment, and adjuvant therapies may be considered for high-risk cases. However, the prognosis remains poor and further research is needed to improve our understanding of the molecular biology of primary renal myoepithelial carcinoma and to develop effective treatment strategies.

#### Ethics Statement

Formal written informed consent was not required with a waiver by the appropriate institutional review board (No. 285/22 MPMCC, Varanasi, India dated 26th December 2022).

#### Availability of Data and Material

Data sharing is not applicable to this article as no datasets were generated or analyzed during the study.

#### Code Availability

Not applicable.

#### ORCID

Nilay Nishith <https://orcid.org/0000-0003-2192-7393>  
Zachariah Chowdhury <https://orcid.org/0000-0002-1766-5012>

#### Author Contributions

Conceptualization: NN, ZC. Writing—original draft: NN. Writing—review & editing: ZC. Approval of final manuscript: all authors.

#### Conflicts of Interest

The authors declare that they have no potential conflicts of interest.

#### Funding Statement

No funding to declare.

#### Acknowledgments

We would like to extend our sincere gratitude to our Dean and In-charge of Molecular Pathology, Dr. Shashikant Patne, and the technical staff of Department of Onco-Pathology for their relentless support.

#### References

1. Jo VY. Soft tissue special issue: myoepithelial neoplasms of soft tissue: an updated review with emphasis on diagnostic considerations in the head and neck. *Head Neck Pathol* 2020; 14: 121-31.
2. She YH, Chen YT, Huang YM, et al. Primary renal myoepithelial carcinoma with *EWSR1* gene rearrangement: case report and literature review. *Acta Nephrol* 2021; 35: 105-11.
3. Cajaiba MM, Jennings LJ, Rohan SM, et al. Expanding the spectrum of renal tumors in children: primary renal myoepithelial carcinomas with a novel *EWSR1-KLF15* fusion. *Am J Surg Pathol* 2016; 40: 386-94.
4. Li Q, Mou Z, Yang K, Jiang H. A first case report of primary epithelial myoepithelial carcinoma-like renal tumor showing a perivascular pseudorosette-like pattern: description of morphologic, immunohistochemical, and genetic features. *Medicine (Baltimore)* 2019; 98: e17245.
5. Yue D, Feng W, Ning C, Han LX, YaHong L. Myoepithelial carcinoma of the salivary gland: pathologic and CT imaging characteristics (report of 10 cases and literature review). *Oral Surg Oral Med Oral Pathol Oral Radiol* 2017; 123: e182-7.
6. Hiyama T, Kuno H, Sekiya K, Oda S, Kobayashi T. Imaging of malignant minor salivary gland tumors of the head and neck. *Radiographics* 2021; 41: 175-91.
7. Hornick JL, Fletcher CD. Myoepithelial tumors of soft tissue: a clinicopathologic and immunohistochemical study of 101 cases with evaluation of prognostic parameters. *Am J Surg Pathol* 2003; 27: 1183-96.
8. Antonescu CR, Zhang L, Chang NE, et al. *EWSR1-POU5F1* fusion in soft tissue myoepithelial tumors: a molecular analysis of sixty-six cases, including soft tissue, bone, and visceral lesions, showing common involvement of the *EWSR1* gene. *Genes Chromosomes Cancer* 2010; 49: 1114-24.
9. Brandal P, Panagopoulos I, Bjerkehagen B, Heim S. t(19;22)(q13;q12) Translocation leading to the novel fusion gene *EWSR1-ZNF444* in soft tissue myoepithelial carcinoma. *Genes Chromosomes Cancer* 2009; 48: 1051-6.
10. Agaram NP, Chen HW, Zhang L, et al. *EWSR1-PBX3*: a novel gene fusion in myoepithelial tumors. *Genes Chromosomes Cancer* 2015; 54: 63-71.
11. McConnell BB, Yang VW. Mammalian Kruppel-like factors in health and diseases. *Physiol Rev* 2010; 90: 1337-81.
12. Uchida S, Tanaka Y, Ito H, et al. Transcriptional regulation of the *CLC-K1* promoter by myc-associated zinc finger protein and kidney-enriched Kruppel-like factor, a novel zinc finger repressor. *Mol Cell Biol* 2000; 20: 7319-31.

